Universidade de Trás-os-Montes e Alto Douro

Role of mitochondrial p66Shc in nefazodone-induced mitochondrial toxicity on HepG2 cells

Dissertação de Mestrado em Biologia

Ana Marta Ribeiro da Silva

Orientador: Doutor Paulo Oliveira.

Coorientador: Doutor Dario Santos.

Vila Real, 2015

Universidade de Trás-os-Montes e Alto Douro

Role of mitochondrial p66Shc in nefazodone-induced mitochondrial toxicity on HepG2 cells

Dissertação de Mestrado em Biologia

Ana Marta Ribeiro da Silva

Orientador: Doutor Paulo Oliveira.

Coorientador: Doutor Dario Santos.

Composição do Júri:

_____

_____

_____

Vila Real, 2015

Orientador

Doutor Paulo Jorge Gouveia Simões da Silva Oliveira

Centro de Neurociências e Biologia Celular, UC

Coorientador

Doutor Dario Joaquim Simões Loureiro dos Santos

Departamento de Biologia e Ambiente, UTAD

Work performed in Mitochondrial Toxicology and Experimental Therapeutics Group, at the Center for Neuroscience and Cell Biology, University of Coimbra, under supervision of Dr. Paulo Oliveira and Dr. Dario Santos.

The work was also performed under the guidance of Dr. Inês Barbosa.

This work was supported by the Portuguese Foundation for Science and Technology (FCT) and co-funded by COMPETE/FEDER/National budget (PTDC/SAU TOX/117912/2010 and PEst-C/SAU/LA0001/2013-2014).

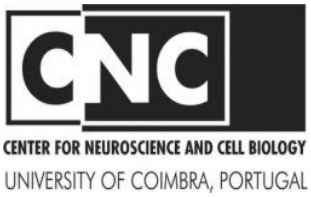

.

This original research was developed to achieve the Master Degree in Biology.

I declare that this is a true copy of my thesis including any final revisions, as approved by my thesis committe, and that this thesis has not been submitted for a higher degree to any other University or Institution.

Ana Marta Silva, BSc

March, 2015

"I was taught that the way of progress was neither swift nor easy."

Marie Curie

Acknowledgments

At the end of another cycle, I could not fail to thank all those who made possible the realization of this project.

Firstly, I want to thank to the entities involved in the financing of this project, supported by Foundation for Science and Technology (FCT) and co-funded COMPETE/FEDER/National budget (PTDC/SAU-TOX/117912/2010 and PEst-C/SAU/LA0001/2013-2014).

I would like to express my sincere acknowledgments to my supervisor, Doctor Paulo Oliveria, for the opportunity to develop this project and for having received me in your group. I appreciate all the words of encouragement throughout this period, which was not always easy. Thank you for all the availability and help in solving all the difficulties associated with this work.

Then, I would like to express my sincere acknowledgments to Doctor Dario Santos for leading me to the opportunity to participate in this project. Thank you for having encouraged me to pursue my goals and for all the things you taught me during the last years.

To all the members of Mitochondrial Toxicology and Experimental Therapeutics Group, for all the help you have given me throughout this work. Thank you for always being available and for sharing your knowledge with me.

To Doctor Inês Barbosa, for all the help provided during this work. Thank you for the availability to teach me and especially for all the encouragement words and for making me believe it was possible to get here.

To all my friends, the best in the world, thank you for having me encouraged along this year. I would like to thank in a special way to Ana Fonseca, Filipa Soares and André Teixeira for always having a kind word to make everything simpler.

Finally, a very special acknowledgment to my family for always been the support that makes all steps surmountable. A very special thank you to my parents for always encouraging me to follow my dreams and understand my passion for science. A special thanks to grandfather Fernando that even far always takes care of me.

Agradecimentos

No final de mais um ciclo, não poderia deixar de agradecer a todos os que tornaram possível a concretização deste projecto.

Em primeiro lugar, quero agradecer às entidades envolvidas no financiamento deste projecto, suportado pela Fundação para a Ciência e Tecnologia (FCT) e co-financiado pelos fundos COMPETE/FEDER/National budget (PTDC/SAU-TOX/117912/2010 and PEst-C/SAU/LA0001/2013-2014).

Agradeço ao meu orientador, o Doutor Paulo Oliveira, pela oportunidade de desenvolver este projecto e por me ter recebido no seu grupo. Agradeço todas as palavras de incentivo ao longo deste período, que nem sempre foi fácil. Muito obrigada por toda a disponibilidade e ajuda na resolução das dificuldades associadas a este percurso.

Em seguida, agradeço ao Doutor Dario Santos por ter sido o elo de ligação a este projecto e pela confiança depositada nas minhas capacidades de trabalho. Obrigada por me ter encorajado a perseguir os meus objectivos e por todos os ensimanentos que me transmitiu ao longo destes anos.

Agradeço a todos os elementos do grupo Mitochondrial Toxicology and Experimental Therapeutics por toda a ajuda que me prestaram ao longo deste trabalho. Obrigada por estarem sempre disponíveis e por partilharem comigo os vossos conhecimentos.

Agradeço especialmente à Dr.ª Inês Barbosa, por ter seguido mais de perto o meu trabalho e me ter ajudado sempre que foi necessário. Obrigada por todas as palavras de incentivo e por sempre me teres feito acreditar que era possível chegar até aqui.

A todos os meus amigos, os melhores do mundo, agradeço por me terem encorajado ao longo deste percurso. Gostaria de agradecer de um modo particular à Ana Fonseca, à Filipa Soares e ao André Teixeira por terem sempre uma palavra amiga para tornar tudo mais simples.

Por fim, agradeço à minha família por ter sido sempre o suporte que torna todas as etapas ultrapassáveis. Um obrigada muito especial aos meus pais por me encorajarem sempre a seguir os meus sonhos e por entenderem a minha paixão pela Ciência. Um obrigada especial ao avô Fernando, que mesmo longe, toma sempre conta de mim.

Abstract

Nefazodone (NEF) is an antidepressive agent that has been used for several years in the treatment of depression. Despite its efficacy in the treatment of depression, NEF was withdrawn from the market after the development of hepatic injury on several patients upon treatment. p66Shc signalling, which implicates its phosphorylation in ser36 residue (pSer36-p66Shc) upon stress stimuli, has been described to be involved on reactive oxygen species (ROS) generation and cell death. After its phosphorylation p66Shc is thought to be translocated to mitochondria where it leads to further ROS production, disrupting mitochondrial function and possibly triggering of cell death.

The main objective of the present work was to investigate whether p66Shc signalling is activated during NEF treatment of a human hepatocellular cell line (HepG2).

Our results revealed an increase on p66Shc content after 72 h of incubation with NEF, whereas, surprisingly the content of p66Shc phosphorylated form was decreased after NEF treatment. Although this study was not able to prove the existence of a link between NEF administration and p66Shc activation and consequent translocation to mitochondria, our results support the existence of a link between NEF treatment and apoptosis in the hepatic cell model. NEF treatment led to a decrease in cell mass, mitochondria depolarization and to changes on HepG2 cell morphology, which showed features typical from apoptotic cells. We also found other evidences supporting apoptosis activation upon Nefazodone treatment, such as the increase on late apoptotic cell population, the decrease on viable/early apoptotic cells and an increase of caspases activity. In summary, our data showed an increase of ROS levels upon NEF treatment which although might be associated with p66Shc signaling and its consequent translocation to mitochondria, the fast turn-over of pSer36-p66Shc may be masking these observations.

Keywords: Apoptosis, Hepatotoxicity, Human hepatocellular liver carcinoma cell line, Nefazodone, p66Shc.

Resumo

A Nefazodona (NEF) é um fármaco antidepressivo, usado durante um longo período no tratamento da depressão. Apesar da sua eficácia, este fármaco foi retirado do mercado devido ao aparecimento de diversos casos de lesão hepática em pacientes submetidos a tratamento com NEF. A via de sinalização celular que envolve a proteína p66Shc, e a sua fosforilação na serina 36 (Ser36) após estimulo de stress, foi anteriormente associada à produção de espécies reactivas de oxigénio e à ocorrência de morte celular. De acordo com esta hipótese, a proteína p66Shc é translocada para a mitocôndria após uma situação de stress celular onde participa na produção de ROS, levando ao comprometimento da função mitocondrial e podendo, ainda, desencadear o processo de morte celular.

O principal objectivo deste trabalho foi investigar a possibilidade de que esta via de sinalização seja activada na linha celular do carcinoma hepatocelular humano (HepG2) durante o tratamento com NEF.

Os resultados obtidos revelaram um aumento do teor de p66Shc em células expostas à nefazodona por um perídodo de 72 h e ainda um surpeendente decréscimo da forma fosforilada desta proteína após o tratamento com NEF. Embora este trabalho não possa comprovar a existência de uma ligação entre a administração de NEF e a activação e translocação da proteína p66Shc, os resultados obtidos corroboram a existência de uma associação entre o tratamento com NEF e o início do processo apoptótico no modelo celular utilizado. O tratamento com NEF levou à diminuição da massa celular, à despolarização mitocondrial e ainda a alterações na morfologia celular, com as células HepG2 a exibirem caracteristicas tipicamente encontradas em células apoptóticas. Foram também encontradas outras evidências consistentes com a activação da apoptose induzida por NEF, como o aumento da população de células apoptóticas, a diminuição da população de células viáveis e o aumento da actividade das caspases. Em suma, os resultados obtidos mostram um aumento dos níveis de ROS após o tratamento com NEF, embora a possibilidade de uma associação entre este aumento e a activação da p66Shc e translocação para a mitocôndria possa estar ocultada devido ao rápido processamento da forma fosforilada da proteína p66Shc.

Palavras-chave: Apoptose, Hepatotoxicidade, linha celular do carcinoma hepatocelular humano (HepG2), Nefazodona, p66Shc.

Table of Contents

List of figures

List of Tables

Abbreviations

ADP	Adenosine diphosphate
ALT	Alanine Aminotransferase
APAF-1	Apoptotic protease activating factor-1
AST	Aspartate Aminotransferase
ATP	Adenosine triphosphate
BAD	BCL-2 associated agonist of cell death
BAK	BCL-2 antagonist/killer
BAX	BCL-2 associated X protein
BCA	Bicinchoninic Acid Assay
BCL-2	B-cell lymphoma-2
BCL2A1	B-cell lymphoma 2-related protein A1
BCL-w	BCL-2-like protein 2
BXL-XL	B-cell lymphoma extra large
BID	BH3 interacting domain death agonist
BIK	BCL-2-interacting killer
BIM	BCL2-like 11
BMF	BCL-2 modifying factor
CAM	Calcein acetoxymethyl ester
CHAPS	3-[(3-Cholamidopropyl)dimethylammonio]-1-propanesulfonate hydrate

CYP3A4	Cytochrome P450 3A4
Cyt c	Cytochrome c
DA	Dopamine
DISC	Death-inducing signaling complex.
DMEM	Dulbecco's modified Eagle's medium
DMSO	Dimethyl sulfoxide
DNA	Deoxyribonucleic acid
DTT	Dithiothreitol
EDTA	Ethylenediaminetetraacetic acid
FASL	Fas ligand
GSH	Reduced Glutathione
GSSG	Oxidized Glutathione
HEPES	(4-(2-hydroxyethyl)-1-piperazineethanesulfonic acid)
HepG2	Human Hepatocellular Carcinoma cell line
HRK	Harakiri, BCL-2 interacting protein
H_2O_2	Hydrogen peroxide
5-HT	5-hydroxytryptamine (serotonin)
5-HT2A	5 hydroxytryptamine (serotonin) (5-HT) receptor 2
IMS	Intermembrane Space
MCL-1	Myeloid cell leukemia 1 protein
MEFs	Mouse embryo fibroblasts
MOAs	Monoamine Oxidase Inhibitors

MOMP	Mitochondrial outer membrane permeabilization
mtHsp70	Mitochondrial heat-shock protein 70
NE	Norepinephrine
NEF	Nefazodone
NOXA	Noxa phorbol-12-myristate-13-acetate-induced protein 1
OMM	Outer mitochondrial membrane
OXPHOS	Oxidative Phosphorylation
PARP	Poly (ADP) ribose polymerase
PBS	Phosphate buffered saline
PI	Propidium iodide
Pin 1	Prolyl isomerase 1
PKC-β	Protein kinase C beta
PP2A	Protein serine/threonine phosphatase type 2
PTB	Phosphothyrosine Binding Domain
PTP	Permeability Transition Pore
PUMA	p53-upregulated modulator of apoptosis
PVDF	Polyvinylidene difluoride
ROS	Reactive Oxygen Species.
SDS	Sodium dodecyl sulphate
SDS-PAGE	SDS-polyacrylamide gels
SHC	Src homolog and collagen homolog proteins
SNaRIs	Serotonin Noradrenergic Reuptake Inhibitors

SOD	Superoxide dismutase
SRB	Sulforhodamine B
SSRIs	Selective serotonin reuptake inhibitors
TCAs	Tricyclic antidepressants
TMRM	Tetramethylrhodamine, Methyl Ester
TNFR	Tumor necrosis factor receptor
TOM/TIM	Outer membrane translocase/inner membrane translocase
TRAIL	Tumor necrosis factor-related apoptosis-inducing ligand
$\Delta\psi m$	Inner mitochondrial membrane potential
Δp	Proton motive force

1. Introduction

1.1. Nefazodone as an antidepressive agent

Nefazodone (NEF) is a phenylpiperazine derivative with a structure similar to trazodone (Lucena et al. 2003) (Fig.1). This drug was approved in 1994 in the United States for the treatment of depression (von Moltke et al. 1999), a common mental disorder, characterized by sadness, loss of interest or pleasure, feelings of guilt or low self-worth, disturbed sleep or appetite, feelings of tiredness, and poor concentration (World Health Organization, 2014).

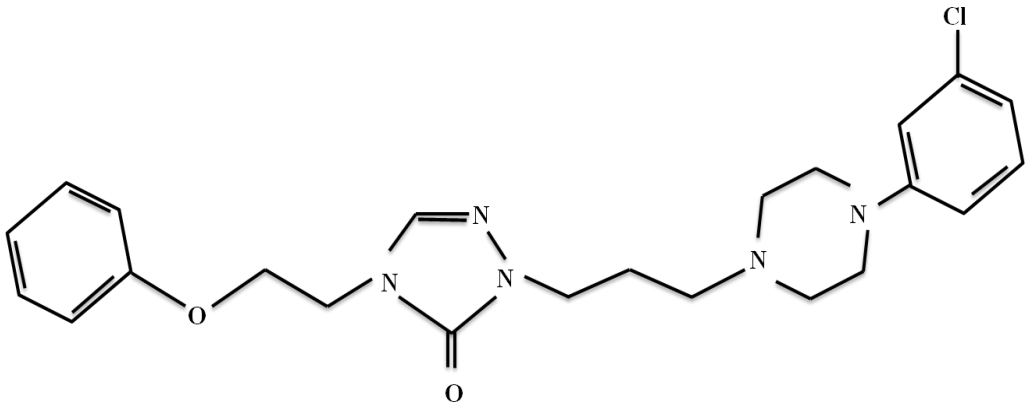

Figure 1: Chemical structure of Nefazodone (Adapted from von Moltke et al. 1999).

Nefazodone belongs to a new generation of antidepressants, alternative to the monoamine oxidase inhibitors (MAOIs), tricyclic antidepressants (TCAs), and serotonin selective reuptake inhibitors (SSRIs).

The MAOIs increase the levels of neurotransmitters such as norepinephrine and serotonin through the inhibition of monamine oxidase, a mitochondrial enzyme capable of metabolizing the mentioned neurotransmitters (He & Richardson 1997). However, side effects such as hepatotoxicity and the need for dietary restrictions to reduce the risk of developing severe hypertensive crises related to the effects of dietary tyramine (Liu & Rustgi 1987; Kent 2000) make this class of antidepressants less used in the present.

The TCAs have several pharmacological targets, such as α-adrenergic receptors and histamine receptors (Horst & Preskorn 1998), causing unwanted side effects which include

dry mouth, sedation, cardiovascular toxicity or postural hypotension (Horst & Preskorn 1998; Kent 2000; Lucena et al. 2003). Unlike the above mentioned compounds, a third class of antidepressants was developed in order to overcome these unwanted side effects: serotonin selective reuptake inhibitors (SSRIs), acting by blocking serotonin uptake at all serotonergic synapses and soon achieving a central role in the treatment of depression (Horst & Preskorn 1998). This class of antidepressants showed clear advantages over TCAs and MOAs regarding safety tolerance and easy of dosing (Kent 2000). Despite these advantages, SRRIs side effects include restlessness, nervousness, insomnia, nausea, diarrhea, agitation and weight gain (Kent 2000), which compromise their tolerance in a patient with depressive condition.

As an alternative to avoid all the unwanted side effects of the previously mentioned antidepressants, another class has emerged: the serotonin noradrenergic reuptake inhibitors (SNaRIs) (Kent 2000). Nefazodone belongs to this class and appeared as a substitute of trazodone, lacking unwanted side effects of trazodone such as excessive sedation and postural hypotension (Kent 2000). Despite being related to trazodone, NEF presents several advantages as it has the capacity to be effective against anxiety and agitation symptoms associated with depression (Taylor & Prather 2003) and also can be used in the treatment of panic disorder (Bystritsky et al. 1999).

Nefazodone mechanism of action is based on its antagonistic activity on post-synaptic 5 hydroxytryptamine (serotonin) (5-HT) receptor 2 (5-HT2A) and also on the inhibition of serotonin and noradrenaline reuptake (Fig.2) (Feighner 1999; Richelson 2001; Ciraulo et al. 2010). According to the monoamine hypothesis for depression, deficience of the biogenic amine system (norepinephrine and/or serotonin pathways) has a central role in the development of a depressive condition (He & Richardson 1997; Hirschfeld 2000). Thus, depressive symptoms are the result of low levels of monoamine neurotransmitters like serotonin (5-HT), norepinephrine (NE), and/or dopamine (DA) (Mulinari 2012; Mahar et al. 2014). Taking this information into consideration, the beneficial effect of NEF in the treatment of depression would result from its capacity to increase serotonin (5-hydroxytryptamine -5-HT) neurotransmission mediated by 5HT1A (Taylor & Prather 2003). The effect of NEF on other neurotransmitters receceptors is limited (Taylor et al. 1986), which allows for a low incidence of side effects upon treatment with this antidepressant.

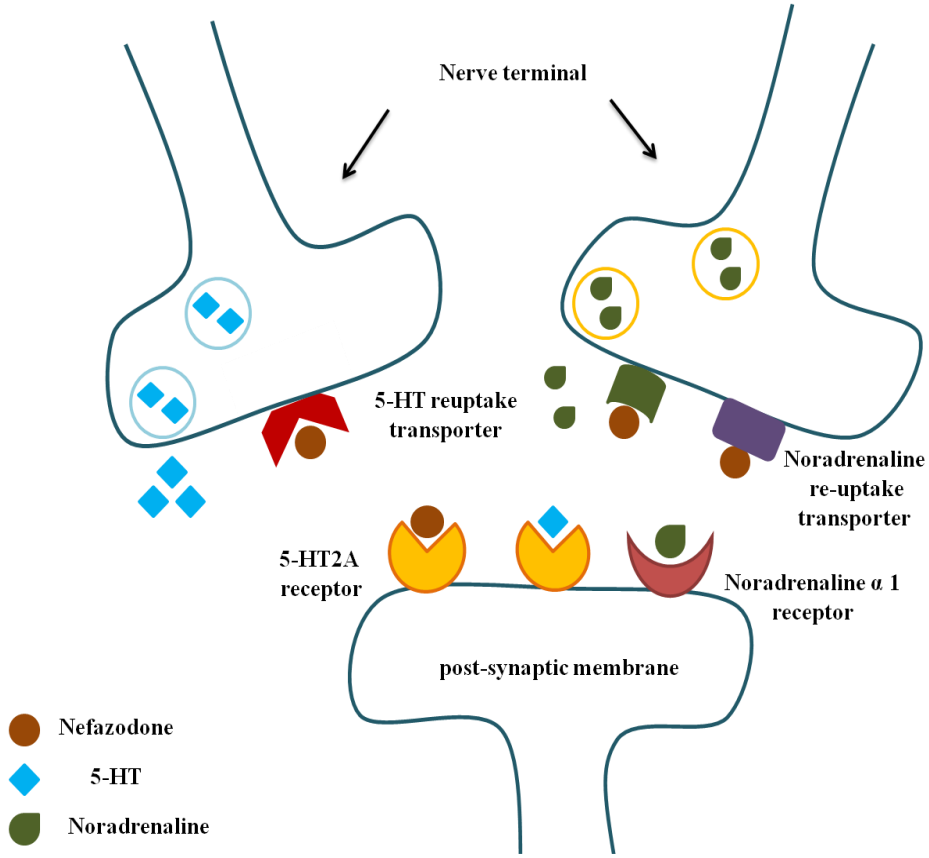

Figure 2: Schematic representation of possible NEF mechanism as an antidepressant. NEF mechanism of action is based on the monoamine hypothesis that suggests a decrease on monoamine neurotransmitters (norepinephrine, serotonin) as the main cause of depression development. Thus, NEF acts as an antagonist on 5-HT2A receptors located on post-synaptic membranes. In addition, NEF also inhibits 5-HT reuptake on pre-synaptic membranes. NEF enhances serotonin neutransmission allowing a successful treatment for depression. (Adapted from CNS forum. The Lundbeck Institute, 2014).

1.2. Nefazodone: drug-induced hepatotoxicity

In 1999, a total of four cases of hepatic injury were reported in patients treated with NEF (Aranda-Michel et al. 1999; Lucena et al. 1999). Later, in 2004, Bristol-Myers Squibb decided to stop the marketing of the drug in the United States as a consequence of the emergence of several hepatotoxicity cases following depression treatment (Aranda-Michel et al. 1999; Eloubeidi et al. 2000; Choi 2003). As a consequence of NEF tretament, hepatotoxic-related symptoms such as jaundice, dark urine, clay colored stool and an increase in the levels of Alanine Aminotransferase (ALT), Aspartate Aminotransferase (AST), total bilirubin level and prothrombin time became common (Aranda-Michel et al. 1999; Lucena et al. 1999) . The toxicity associated with NEF has been described as idiosyncratic (Cosgrove et al. 2009),

which means that adverse effects were not verified in the majority of people treated with the range of doses used clinically. This fact constitutes a restriction in the investigation of drug-toxicity. Another limitation regarding the study of the observed NEF-induced toxicity is associated with the fact that both cell and animal models are inefficient in its detection. Consequently, the majority of idiosyncratic drug hepatotoxicities are not identified before the approval for human use (Cosgrove et al. 2009).

A proposed mechanism for NEF's hepatotoxicity is based on the metabolism of the drug. This hypothesis came out due to the fact that, although NEF is metabolized by cytochrome P450 3A4 (CYP3A4) it also acts as an inhibitor of this enzyme, which may lead to several interactions with other xenobiotics, each with their own mitochondrial liabilities (Benazzi 1997; Alderman 1999). Nefazodone toxicity also interferes with normal mitochondrial function. During the development of a new approach to evaluate mitochondrial toxicity of several drugs, Nadacaniva et al. verified that at a concentration of 50 μM, NEF strongly inhibits complex I of oxidative phosphorylation (OXPHOS). However, the drug also inhibited complexes II+III, IV and V (Nadanaciva et al. 2007). The inhibitory effect of NEF on OXPHOS complexes was also verified in experiments developed by Dykens et. al, reforcing the potently inhibition of complex I by NEF, on isolated bovine heart mitochondria (Dykens et al. 2008). In this study, the toxic effect of NEF at the mitochondrial level was supported by other data suggesting that NEF impairs normal mitochondrial membrane potential, markedly reducing intracellular reduced glutathione and increasing reactive oxygen species (ROS) generation on primary cultures of human hepatocytes. A dramatic reduction on oxygen comsumption on isolated rat liver mitochondria was also identified (Dykens et al. 2008).

Alterations on OXPHOS complexes can compromise cell survival, attending that OXPHOS is the major source of cellular energy, provided by mitochondria (Nadanaciva et al. 2007).

1.3. Cell Death Signaling Pathways

Apoptosis, or programmed cell death, has a central role in the development and homeostasis of all multicellular organisms (Jacobson et al. 1997; Horvitz 1999). This form of cell death was first described by Kerr and colleagues in 1972 (Kerr et al. 1972) and is triggered in response to physiologic or pathologic stimuli (Hengartner 2000). The apoptotic process is essential for normal development (Tebourbi et al. 1998) and is under strict regulation. A failure in this control can lead to the development of pathological conditions as the supression of the apoptotic machinery, described to be responsible for the development of autoimmune diseases, and constituting a cancer hallmark (Thompson 1995; Hanahan & Weinberg 2000). Apoptotic cells show typical features such as cytoplasmic membrane blebbing, chromatin condensation, deoxyribonucleic acid (DNA) fragmentation, disruption of organelle membranes, mitochondria disruption and apoptotic bodies generation (Kerr et al. 1972; Trump et al. 1997; Savill & Fadok 2000). Another feature of apoptosis is the absence of inflammatory reaction, due to phagocytosis of apoptotic cells by macrophages and adjacent cells, avoiding the release of cell content (Savill & Fadok 2000; Kurosaka et al. 2003).

Two main apoptotic pathways have been described so far, the extrinsic pathway (or death receptor pathway) and the intrinsic pathway (or mitochondrial pathway). These two pathways are linked so that molecules in one pathway can influence the other (Igney & Krammer 2002). Both pathways converge to caspase-3 and other proteases and nucleases that drive the latest events of programmed cell death (Jin & El-deiry 2005).

1.3.1.Extrinsic Apoptotic Pathway

The extrinsic pathway of apoptosis (Fig.3-A) involves cell surface death receptors such as Fas, tumor necrosis factor receptor (TNFR) or tumor necrosis factor-related apoptosis-inducing ligand (TRAIL) receptors (Jin & El-deiry 2005). Fas receptor is stimulated through the binding of Fas ligand (FASL), leading to the recruitment of the adaptor protein Fas-associated death domain (FADD) and caspase-8. Together, these components form the death-inducing signaling complex (DISC) which is involved in the autoactivation of initiator caspase-8 and the begining of a caspases cascade, with the activation of effector caspases -3,

-6 and -7 and progression of the apoptotic process (Nagata & Golstein 1995; Lee et al. 1997; Jin & El-deiry 2005).

1.3.2. Intrinsic Apoptotic Pathway

The intrinsic apoptotic pathway (Fig.3-B) can be triggered by several intrinsic signals such DNA damage, cytotoxic stress, cytokine deprivation, (Brenner & Mak 2009) viral infection or growth-factor deprivation (Youle & Strasser 2008). B-cell lymphoma-2 (BCL-2) family of proteins plays an important role in the regulation of the intrinsic pathway as well as in the maintenance of mitochondrial integrity (Cory & Adams 2002; Youle & Strasser 2008). This family of proteins includes pro-apoptotic and anti-apoptotic elements (Elmore 2007; Yao et al. 2012).

Both BAX and BAK are pro-apoptotic proteins involved in a major event of the intrinsic apoptotic pathway, the mitochondrial outer membrane permeabilization (MOMP) (Brenner & Mak 2009). One of the hypothesis that explains BAX and BAK role in MOMP suggests that these proteins form pores in the outer mitochondrial membrane (OMM) (Mikhailov et al. 2003) allowing the release of cytochrome c (cyt c) and other apoptotic factors from mitochondria to the cytoplasm. Consequently, cytoplasmic cyt c interacts with and binds to the apoptotic protease activating factor-1 (Apaf-1) and to pro-caspase 9, resulting in the formation of the apoptossome, a complex responsible for the conversion and activation of pro-caspase 9 into caspase-9 (Zou et al. 1999; Acehan et al. 2002). This activation triggers a cascade of caspases with the subsequent activation of executioner caspases -3 and -7 (Li et al. 1997). Once activated, effector caspases allow the apoptotic process through protein cleavage (Mennella 2011). Nuclear lamins (Lazebnik et al. 1995), retinoblastoma (Janicke et al. 1996) and DNA dependent protein kinase (Casciola-Rosen et al. 1996) are some of the target proteins cleaved by caspases.

In addition to BAX and BAK, another group of pro-apoptotic proteins have been described, including BAD, BIK, BID, HRK, BIM , BMF, NOXA and PUMA. These pro-apoptotic proteins share a sequence of amino acids called BH3 domain (BH3-only proteins). Two different hypothesis have been proposed to explain the mechanism through which BH3-only proteins promote apoptosis. One of the models proposes that this class of proteins directly binds to and inhibits BCL-2 anti-apoptotic proteins, allowing BAX and BAK to allow

the release of cyt c and other intermembrane proteins (Willis et al. 2007). In this model, BCL-2 anti-apoptotic proteins are sequestred by BH3-only proteins, blocking the ability of BCL-2 anti-apoptotic proteins to neutralize BAX and BAK action, and allowing the permeabilization of the OMM, as previously mentioned (Willis et al. 2007). An alternative model suggests that BH3-only proteins are involved in the direct activation of BAX and BAK pro-apoptotic proteins (Youle 2007). When activated, BAX and BAK can insert and oligomerize into the OMM allowing permeabilization and the release of cyt c to the cytoplasm, triggering the activation of the intrinsic/mitochondrial apoptotic pathway (Wei et al. 2001; Youle et al. 2007; Youle & Strasser 2008).

As mentioned above, the BCl-2 family also includes anti-apoptotic proteins, such as BCL-2, BCL-XL, MCL-1, BCL-w and BCL2A1, which act by binding to pro-apoptotic proteins keeping them in an inactive form (Brenner & Mak 2009).

The balance between the pro-apoptotic and anti-apoptotic proteins has a key role in determining whether the cell undergoes apoptosis or not.

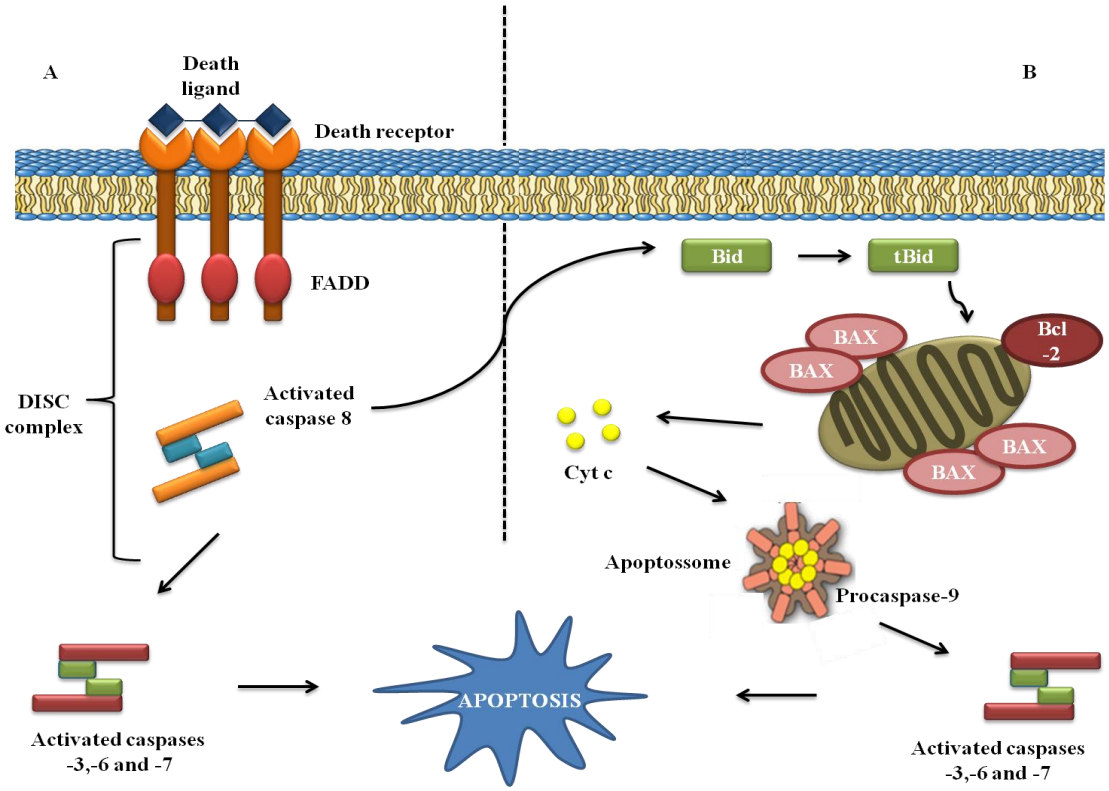

Figure 3: Extrinsic and intrinsic apoptotic pathways. The extrinsic apoptotic pathway (A) is triggered in response to the binding of extracellular signalling proteins to cell surface death receptors, such as Fas, TNFR or TRAIL receptors. These transmembrane proteins are formed by three domains: an extracellular ligand-binding domain, a transmembrane domain and an intracellular death domain, involved in the progression of the apoptotic process. The receptors and the ligands are both homotrimers and structurally related. The binding of Fas receptor to FASL, stimulates receptor trimerization and the recruitment of the adaptor protein Fas-associated death domain (FADD) and caspase-8. These elements form the death DISC complex, responsible for the autoactivation of initiator caspase-8 which in turn results in the initiation of a caspases cascade, which included the activation of executioner caspases-3, -6 and -7, downstream effectors of the cell death program (Ashkenazi & Dixit 1998; Nagata et al. 1995; Jin & El-deiry 2005) . The intrinsic apoptotic pathway (B) can be activated in the presence of an intrinsic signal, such as DNA damage, cytotoxic stress, cytokine deprivation, viral infection or growth-factor deprivation (Elmore 2007; Parsons & Green 2010). In the presence of apoptotic stimulus, the proteins BAX and BAK form oligomers on the OMM, allowing the release of cyt c and other pro-apoptotic proteins from the intermembrane space to cytosol (Brenner & Mak 2009). The mechanism by which this release occurs remains unclear. Once in the cytosol, cyt c forms a complex with Apaf-1 and pro-caspase 9, known as "apoptossome", where the pro-caspase 9 is activated giving rise to caspase-9. This process initiates a cascade of caspases, resulting in the activation of -3, -6 and -7 caspases (Zou et al. 1999). As a consequence of caspases activation, the apoptotic process is promoted through protein cleavage. Nuclear lamins (Lazebnik et al. 1995), retinoblastoma (Janicke et al. 1996) and DNA dependent protein kinase (Casciola-Rosen et al. 1996) are some of the target proteins cleaved by caspases. t-BID, a BH3-only protein, is responsible for connecting the extrinsic and intrinsic apoptotic pathways. When the extrinsic pathway is triggered, caspase-8 cleaves BID protein, generating a truncated form, t-BID, that is translocated to mitochondria. In mitochondria, t-BID inhibits BCL-2 anti-apoptotic proteins and promotes the agregation of BAX and BAK pro-apoptotic proteins on the OMM and the consequent release of cyt c (Li et al. 1998). This interaction between the two apoptotic pathways allows the death signal to be amplified (Adapted from Cooper 2012).

1.4. p66Shc in ROS Generation and Cell Death

p66Shc protein belongs to Src homolog and collagen homolog protein (Shc) family, that are adapter proteins with a typical domain organization: a phosphotyrosine binding domain (PTB), a collagen homology 1 (CH1) region, and an Src homology 2 (SH2) domain (Migliaccio et al. 1997) (Fig.4). Besides these three domains, p66Shc also presents an additional N-terminal proline-rich CH2 domain, with a serine residue at position 36, that is phosphorylated after a cellular stress stimulus, as explained below (Migliaccio et al. 1997, 1999).

Mammalian Shc *locus* encodes for three different adaptor proteins: p66Shc, p52Shc and p46Shc (Cosentino et al. 2008). While p52Shc and p46Shc induce the Ras signaling pathway, p66Shc, which is mainly expressed in epithelia (Veeramani et al. 2012), acts as a redox enzyme, taking part in mitochondrial ROS generation and translation of oxidative signals into apoptosis (Bonfini et al. 1996; Cosentino et al. 2008).

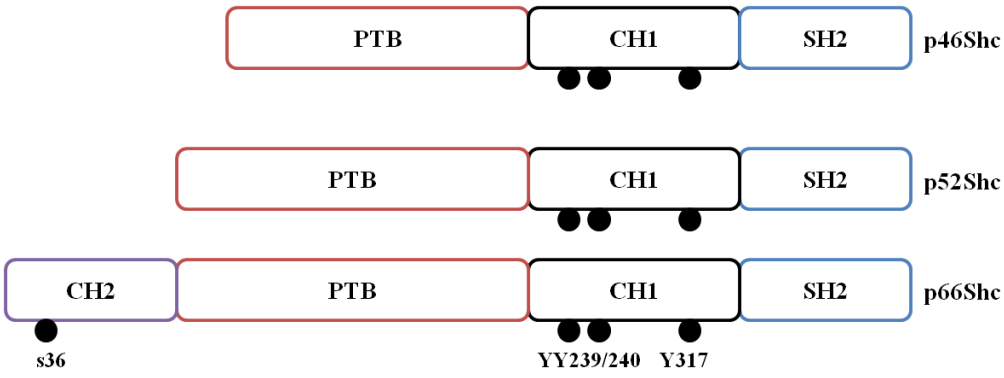

Figure 4: Schematic organization of SHC1 protein isoforms. p46Shc, p52Shc and p66Shc share a similar structure, with a Src homoly domain 2 (SH2), a collagen homology domain 1 (CH1) and a phosphothyrosine binding domain (PTB). p66Shc has another collagen homogy domain (CH2), binding to its PTB domain, with a Serine 36 (s36), represented as a black dot. This serine is phosphorylated in reaction to oxidative damage. Black dots on CH1 domain from the three isoforms represent major tyrosine-phosphorylation sites (YY 239/240; YY317) (Adapted from Luzi et al. 2000).

One of the hypothesis that explains the role of p66Shc in ROS generation and cell death suggests that in the presence of oxidative stress signals, cytoplasmatic p66Shc is translocated to mitochondria (Orsini et al. 2004; Giorgio et al. 2005), due to an interaction with TOM/TIM import complexes and mtHsp70. Once in mitochondria, p66Shc associates

with cyt c, acting as an oxidoreductase allowing ROS generation (Giorgio et al. 2005). The mechanisms by which ROS lead to apoptosis are related to the permeability transition pore (PTP) induction, and involve oxidation-dependent mechanisms (Petronilli et al. 1994; Danial & Korsmeyer 2004). According to this model, PTP opening increases inner membrane permeability to ions and solutes, followed by a consequent water influx into the mitochondrial matrix. This water entrance can cause the swelling of the organelle and the physical rupture of its outer membrane, resulting in the release of proteins of the intermembrane space, including cyt c, (Lindsten et al. 2011) previously described as an apoptotic factor.

As mentioned above, p66Shc is translocated from cytoplasm to mitochondria. The mechanism underlying its entrance to mitochondria involves a set of steps and proteins (Fig.5). Firstly, protein kinase C beta (PKC-β) induces p66Shc phosporylation on Ser 36 (Pinton et al. 2007), which is then recognized by Prolyl isomerase 1 (Pin1) that catalyzes its cis-trans isomeration. After that, serine 36-phosphorylated p66Shc undergoes dephosphorylation by type 2 protein serine/threonine phosphatase (PP2A), and enters to mitochondria. In mitochondria, p66Shc binds to cyt c and acts as an oxidoreductase, shuttling electrons from cyt c to molecular oxygen and increasing ROS levels (Raffaello & Rizzuto 2011).

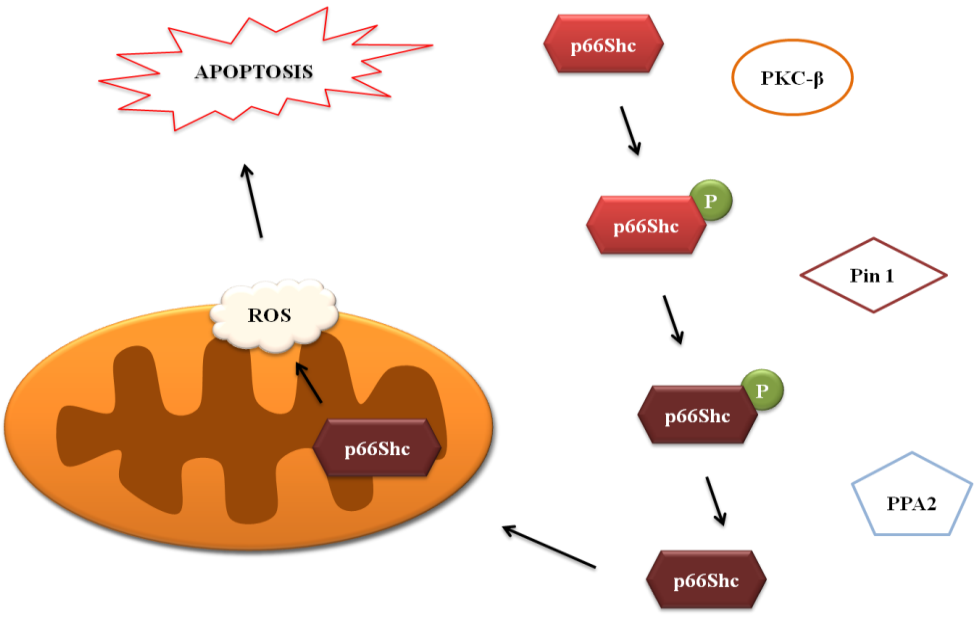

Figure 5: p66Shc-dependent ROS increase. In the presence of oxidative stress signals, such as ROS or Ca^{2+}, p66Shc is phosphorylated on Ser36 by activated PKC-β. Serine 36-phosphorylated p66Shc, is then recognized by Pin1, an enzyme involved in its cis-trans isomeration. After that, Serine 36-phosphorylated p66Shc undergoes dephosphorylation catalyzed by PP2A, and enters mitochondria. Once inside mitochondria, p66shc binds to cyt c, leading to its oxidorreductase activity (Adapted from Raffaello & Rizzuto 2011).

Several authors validated this p66Shc signalling pathway. Giorgio et al. (2005) developed a detailed work focused on the study of different aspects of this pathway. Data obtained suggest that p66Shc can directly stimulate mitochondrial ROS generation. The same work also strongly supports the occurence of electron transfer between cyt c and p66Shc, supporting the action of p66Shc as oxidorreductase. The influence of p66Shc on the permability transition and mitochondria sweeling was also explored in this work, with data suggesting that p66Shc can induce mitochondria swelling.

Pacini et al. (2004) verified that over-expression of p66Shc promoted apoptosis on mouse splenic T-cells exposed to different apoptotic stimulus such as H_2O_2, calcium ionophore A23187 or Fas ligation.

The mechanism proposed for p66Shc in the regulation of ROS generation and cell death is also important to understand the aging process. In 1956, Harnan suggested aging and associated degenerative diseases as a result of free radicals effects on different cell components (Harman 1956). Based on this idea, Migliaccio et al. (1999) performed a study suggesting p66Shc as having an important role in the response to a situation of oxidative stress and in the regulation of lifespan. The author performed experiments using $p66^{shc-/-}$ mice exposed to paraquat (an agent that generates superoxide anion), showing an increase on life span when compared to wild-type mice exposed to the same agent. The same author also observed an increase on $p66^{shc-/-}$ mouse embryo fibroblasts (MEFs) survival when exposed to H_2O_2 and UV radiation, comparatively to wild-type MEFs. These data support the idea of p66Shc as having a central role on the apoptotic response to oxidative damage and also in the regulation of aging process.

1.5. HepG2 cells as a model to study NEF-induced Hepatotoxicity

The human hepatocellular carcinoma (HepG2) cell line (Fig.6) has been commonly used in several studies, due to the ability to keeping a similar cellular function to normal hepatocytes. This cell line exhibits several features similar to those found in normal hepatocytes, such as the ability to synthesize and secrete plasma proteins and the expression of cell surface receptors found in normal hepatocytes, previously described in several works (Roe et al. 1993; Dehn et al. 2004).

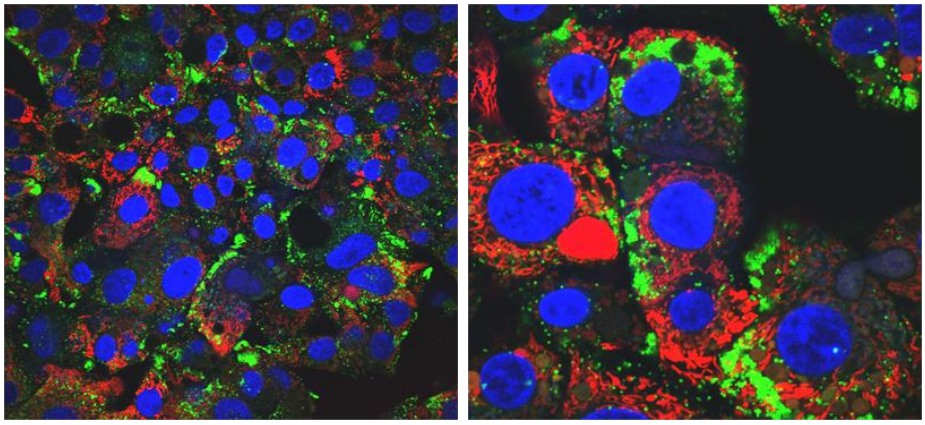

Figure 6: Confocal microscopy images of HepG2 cells labeled with Tetramethylrhodamine, methyl ester (TMRM) (red, mitochondria staining), LipidTOX (green, neutral lipid droplets staining) and Hoechst 33342 (blue, DNA staining). Images gently supplied by Dr. Paulo Oliveira.

The use of HepG2 cell line can also be justified due to its high degree of morphological and functional differentiation *in vitro*, that makes this cell line a proper model for intracellular trafficking, hepatocarcinogenesis, and drug targeting studies *in vitro* (van IJzendoorn & Hoekstra 2000). The cytotoxic effect of NEF on HepG2 cells was already verified by Dykens et al. (2008), showing that the exposure of HepG2 cells to high concentrations of NEF, serious compromise ATP generation, leading to a depletion of ATP. The same work also revealed that HepG2 cells exposed to NEF have decreased on oxygen comsumption, followed by an increase on extra-cellular acidification rate (ECAR) (Dykens et al. 2008). Also, HepG2 cell line was already used by several authors as a model to evaluate other drugs cytotoxicity (Thabrew et al. 2005; Lin & Will 2012).

1.6. Hypothesis

As previously mentioned, NEF hepatotoxicity led to the withdrawal of this drug from the market. In fact, its administration resulted in the occurence of several cases of liver injury, some of which led to the need of liver transplant or resulted in patients death (Aranda-Michel et al. 1999; Lucena et al. 1999). Experimental works have proved that NEF administration can interfere with normal mitochondrial function, through the alteration of OXPHOS complexes activity (Nadanaciva et al. 2007).

In the present work we hypothesize that the activation of p66Shc signaling pathway is involved in the toxicity induced by NEF. This approach, proposing a main role for p66Shc on NEF-induced cell hepatotoxicity has never been explored before.

This hypothesis, proposing a link between exposure to NEF and activation of the p66Shc signalling pathway, may be a valuable tool for researchers and clinicians, allowing to understand if exposure to a particular drug can lead to the establishment of mitochondrial and cellular stress. In order to achieve this, we investigate whether NEF leads to the activation of p66Shc signalling pathway in HepG2 cell line.

.

2. Materials and Methods

2.1. Reagents

Reagents used in cell culture such as Fetal Bovine Serum (FBS; Catalog# 16000-044), trypsin-EDTA (Catalog# 25300-062), Penicillin-Streptomycin (Catalog# 15140-122), were purchased from Invitrogen (Carlsbad, CA, USA). Cell medium used was Dulbecco's Modified Eagle's Medium (DMEM, Catalog# D5648) and purchased from Sigma-Aldrich (St. Louis, MO, USA).

Reagents including Radio Immunoprecipitation Assay Buffer (RIPA buffer; #Catalog R0278), DL-dithiothreitol (DTT, #Catalog D9779), and Protease Inhibitor Cocktail (PIC, #Catalog P8340) were purchased from Sigma-Aldrich (St. Louis, MO, USA).

To determine protein content in samples used on Western-Blot technique, the Pierce BCA assay kit (Catalog# 23250) was purchased from Thermo Fisher Scientific (Lafayette, CO, USA). The primary antibodies also used on Western-Blot analysis are listed on table 1 (dilution, host and supplier) as well as the secondary antibody used,which was obtained from Santa Cruz Biotechnology (Heidelberg,Germany). The unicolor molecular weight standard (Catalog# MB176) was purchased from NZYTech (Lisbon, Portugal) and the non-fat dry milk (Catalog# 170-6404) used as a blotting-grade blocker was purchased from BioRad (Hercules, CA, USA). Additionally, 2x Laemmli Sample Buffer (Catalog# 161-0737) used to prepare samples for Western-Blot analysis was purchased from BioRad (Hercules, CA, USA). Ponceau S (Catalog# P3504), used to confirm equal amounts of protein was obtained from Sigma-Aldrich (St.Louis, MO, USA). Regarding caspases activity, caspases-3 (Catalog# 235400) and -9 substrates (Catalog# 218805) were purchased from Calbiochem (San Diego, CA, USA). pNA (Catalog# 185310) used to method calibration was obtained from Sigma-Aldrich (St. Louis, MO, USA). Bradford Reagent, used to quantify protein for caspases activity assay was also purchased from Sigma-Aldrich (St. Louis, MO,USA).

Fluorescence dyes including Tetramethylrhodamine, methyl ester (TMRM Catalog# T-668), MitoSOX Red (Catalog# M-36008), calcein acetoxymethyl ester (Calcein-AM; Catalog# C1430), and Propidium Iodide (PI, #Catalog 21493), were purchased from Invitrogen (Carlsbad, CA, USA). Hoechst 33342 (Catalog# B2261) was purchased from Sigma-Aldrich (St. Louis, MO, USA).

The drug tested in the present work, nefazodone (NEF; Catalog# N5536) was obtained from Sigma-Aldridch (St. Louis, MO, USA), which was prepared in Dimethyl sulfoxide, also purchased from the same company (DMSO; Catalog# 34869) and kept refrigerated at a stock solution of 19.7 mM. Sulforhodamine B (SRB; Catalog# 9012) reagent was also purchased from Sigma-Aldridch (St. Louis, MO, USA).

2.2. Cell culture and treatment

The HepG2 cell line was kindly provided by Dr. Carlos Palmeira (Center for Neuroscience and Cell Biology, University of Coimbra). Cells were cultured in high glucose Dulbecco's Modified Eagle's Medium (DMEM). This medium was supplemented with 10% fetal bovine serum, 1 mM sodium pyruvate, 1.8 g/L sodium bicarbonate and 1% penicillin-streptomycin, in 60 cm^2 tissue culture dishes at 37°C in a humidified atmosphere of 5% CO_2.

2.3. Sulforhodamine B Colorimetric Assay

Sulforhodamine B colorimetric assay was introduced in 1990 by Skehan (Skehan et al. 1990) and it is based on the ability of SRB to bind to alkaline amino acids of cellular proteins (Papazisis et al. 1997). The pink dye binds to alkaline aminoacid residues under mild acidic conditions and dissociates under alkaline conditions. Through a colorimetric evalution, the assay allows the estimate of the total protein content, which is related to cell number (Papazisis et al. 1997; Longo-sorbello et al. 2006). This assay was performed in order to evaluate NEF cytotoxic effects on HepG2 cells with the main goal of chosing NEF working concentrations for further experiments. To perform this assay, HepG2 cells were seeded in 48 well plates at a desity of $2x10^4$ cells/well. After 24 h, incubation medium was removed and NEF was added in the following concentrations: 0 μM, 5 μM, 10 μM, 20 μM, 50 μM and 100 μM. Different exposure times to NEF were also tested: 0 h, 6 h, 24 h, 48 h and 72 h (Fig.7). A control was done using DMSO (always less than 0.1% v/v).

After the correspondent exposure time, NEF was removed and cells were fixed in 1% acetic acid in ice-cold methanol, for at least 24 h. Cells were then incubated with 0.5% (wt/vol) SRB in 1% of acetic acid for 1 h at 37°C. After the incubation period, the unbound

dye was removed with 1% acetic acid solution. To extract dye bound to cell proteins, a solution of Tris base 10 mM, pH 10, was used. The optical density of the solution was determined at 545 nm, using VICTOR X3 plate reader (Perkin Elmer Inc.).

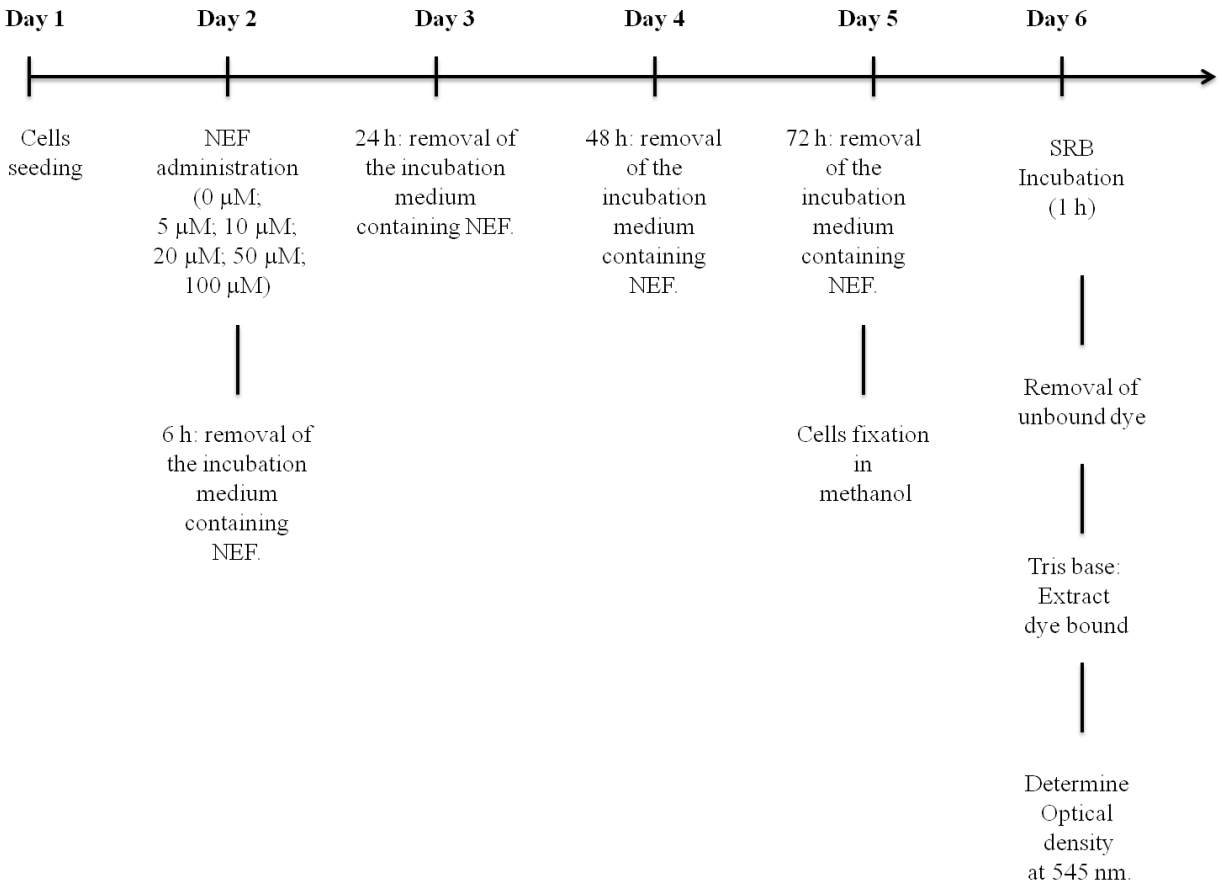

Figure 7: Experimental design for SRB assay. 24 hours after cell seeding, HepG2 cells were incubated with different concentrations of NEF for different time periods in order to evaluate NEF toxicity in this cell line.

2.4. Collection of total Extracts from HepG2 cells

Cells were seeded on 60 cm^2 dishes at a density of $1.7x10^6$ cells/dish. Three different groups were considered to collect protein samples: control group (no NEF added), cells treated with 20 µM NEF and cells treated with 50 µM NEF. The three conditions were tested for two different exposure times, 48 h and 72 h.

After treatment, total cellular extracts were collected according to the following procedure: cells were harvested using a scraper and applying a mixed solution of PBS and Ethylenediaminetetraacetic acid (PBS-EDTA). Two centrifugation steps were then performed for 3 minutes at 300xg. Cellular pellet was ressuspendeded in RIPA buffer (150 mM NaCl, 1.0% IGEPAL® CA-630, 0.5% sodium deoxycholate, 0.1% SDS, and 50 mM Tris, pH 8.0) supplemented with dithiothreitol (DTT) and protease inhibitor cocktail (PIC) according to manufacturers instructions. The cell suspension was stored at -80°C until used.

2.5. Determination of Protein Content for Western-Blot Analysis: Bicinchonic acid assay (BCA)

The protein content of each sample was determined using the bicinchonic acid assay (BCA). This colorimetric method was first introduced by Smith et al. (Smith et al. 1985) and is based on the biuret reaction (Sampson et al. 2013): under alkaline conditions, the protein residues bind and reduce copper ions from cupric ions (Cu^{2+}) to cuprous ions (Cu^{1+}). On a second step of this reaction, two molecules of BCA react with a cuprous ion, producing a purple-colored complex, whose absorbance can be read.

The method was used to evaluate the protein content from control cells, and cells treated with 20 µM and 50 µM NEF for 48 h and 72 h.

To perform this technique, previously collected samples were first sonicated and then diluted in ultrapure water (Merck Millipore, Germany) in a 1:20 dilution. After dilution, 5 µl of each sample, were transferred to a 96-well plate. Protein content was determined by BCA assay, using Bovine Serum Albumin (BSA) as a standard. The reaction was left to occur for 30 minutes at 37°C after which absorbance was read at 545 nm using VICTOR X3 plate reader (Perkin Elmer Inc.).

2.6. Western-Blot Analysis

After quantification, protein samples were then prepared in Laemmli Buffer and denatured at 95°C during 5 minutes. Then, equivalent amounts of proteins (20 µg) were separated by electrophoresis in 10% SDS-polyacrylamide gels (SDS-PAGE composição do gel). Casted gels were fitted in a Mini-PROTEAN 3 Cell (Bio-Rad) filled with running buffer

(25mM Tris, 192mM glycine, 0.1% SDS) and connected to a PowerPac Basic Power Supply (Bio-Rad) outputting a constante voltage of 120V. Separation was carried out at room temperature and until the front of the run reached the bottom end of the gel. Note that in every gel, a molecular weight standard (NZYBlue Protein Marker, from NZYTech) was included to allow molecular weight estimation. After protein separation, transfer was performed to a thin surface layer of pre-activated (5 sec in 100% methanol followed by 5 min in distilled water and 15 min in TBST) polyvinylidene difluoride membrane (PVDF, 0.45µm, Millipore, Billerica, MA, USA). For that, gels were placed in a "transfer sandwich" (filter paper-gel-membrane-filter paper), in a system suported by a cassette. This sandwich system was placed in a Mini Trans-Blot Cell (Bio-Rad) tank between stainless steel/platinum wire electrodes and filled with transfer buffer (25mM Tris, 190mM glycine and 20% methanol). Protein transference was performed during 90 minutes at a constant voltage of 100 V. Membranes were then blocked in 5% milk in Tris-buffered saline Tween-20 (TBS-T; 154 mM NaCl, 50 mM Tris pH 8.0 (HCl) and 0.1% Tween-20) at 4 °C overnight and incubated with the primary antibodies (Table 1) overnight at 4°C under agitation. Membranes were washed with TBS-T and incubated with secondary antibodies (Table 1). Once incubation was finished, membranes were washed three times for 5 minutes each with TBS-T, a step followed by the incubation of membranes with Enhanced Chemi-Fluorescence (ECF) detection system (GE Healthcare, NJ, USA). Membrane imaging was performed using the UVP Biospectrum 500 Imaging System (UVP, Upland, CA, USA). To determine the intensity of each band the VisionWorksLS image aquisition and analysis software was used (UVP, Upland, CA, USA). In order to confirm that each lane was filled with an equal amount of protein, PVDF membranes were stained with Ponceau S (Sigma-Aldrich,St.Louis, MO, USA).

Table 1: Primary and secondary antibodies used for Western Blotting experiments.

Primary Antibodies	Diluition	Host Species	Gel (%)	Supplier
p66Shc	1:1000	Mouse	10	BD Biosciences (#610879)
p66Shc-p (Ser 36)	1:1000	Mouse	10	Calbiochem (#566807)
Secondary Antibodies	**Diluition**	**Host Species**	**Gel (%)**	**Supplier**
Goat anti-mouse IgG-AP	1:2500	Mouse	10	Santa Cruz Biotechnology (#B1714)

2.7. Flow cytometry

HepG2 cells were seeded on 20 cm^2 dishes at a density of $5.7x10^5$/dish. The experimental groups considered on this assay were: control group, cells treated with either 20 µM or 50 µM NEF. These conditions were tested for two different exposure times: 48 h and 72 h.

On the day of the experiment, the culture medium was removed and cells were washed once with a solution of PBS 1x. Cells were then harvested by trypsinization, centrifuged and ressuspended around 500 µl of Hank's Balanced Salt Solution 1x (HBSS-1x), containing of Tetramethylrhodamine, methyl ester (TMRM) at a concentration of 150 nM. Incubation was performed during 30 minutes, in the dark, at 37°C under normal growth conditions. Samples were kept in the dark until used and 20,000 cells were analysed on a FACSCalibur flow cytometer (BD Biosciences, San Jose, California, USA) at a low sample flow rate.

TMRM is a cationic cell permeant and attending to its positive charge it will be accumulated by polarized mitochondria (more negative inside) and less accumulated by depolarized mitochondria. Through this principle, TMRM constitutes a useful tool to semi-quantify the inner mitochondrial membrane potential ($\Delta\psi m$), a component of proton motive force (Δp) (Perry et al. 2011).

2.8. Confocal microscopy

Cells were seeded on 60 cm^2 dishes, at a density of $1.7x10^6$/dish. The experimental groups considered on this assay were: control group, cells treated 20 µM NEF and cells treated with 50 µM. The following conditions were tested for two different exposure times: 48 h and 72 h. Twenty-four hours before the different exposure times were finished, cells were transferred to from dishes to µ-Slide 8 well ibiTreat (ibidi Martinsried, Germany) at a density of 50,000 cells/well. The same experimental groups were maintained. Once treatment period was finished, cell culture medium was removed and cells were incubated with either a TMRM (150 nM) and Hoechst 33342 (1 mg/ml) fluorescent dyes or a mixture of Hoechst (1 mg/ml) and MitoSOX Red mitochondrial superoxide indicator, 5 µM (solutions were prepared on HBSS1x medium). Incubation was performed during 30 minutes at 37°C, protected from light. Cells were observed under a Zeiss LSM 510Meta confocal microscope. Images were obtained through LSM Image Browser. A Diode 405-30 laser (30 mW) at a 2% power was used for Hoechst 33342, while a DPSS 561-10 (15mW) laser was used for TMRM and MitoSOX, at a power of 1% and 2%, respectively. Emission filters BP420-480 and LP575 were used for collecting blue and red channel images, respectively. A EC Plan-Neofluar 40x/1.30 oil DIC lens was used to capture all the images, at a 512x512 pixels resolution. Pinhole was maintained at 74, for both channels. Image acquisition and image analysis was done at the MICC Imaging facility of CNC.

MitoSOX Red was used to evaluate superoxide anion generation in mitochondria from live cells. The use of this dihydroethidium derivative was described previously by several authors (Abramov et al. 2007; Pehar et al. 2007). The assay is based on the capacity of MitoSOX to enter mitochondria due to the presence of a positively charged phosphonium group in this fluorescent dye. Once oxidized by mitochondrial superoxide anion, MitoSOX exhibits red fluorescence (Robinson et al. 2006). In addition, Hoechst 33342, a fluorescent dye, was used to visualize the cell nucleus, due to its ability for binding to DNA (Arndt-Jovin & Jovin 1977; Weisenfeld 2007) .

2.9. Calcein-AM and Propidium Iodide Assay

This assay performed by using Calcein-AM (CAM) and propidium iodide, was performed with the aim of assess cell viability. On intact cells, the active intracellullar esterases are capable to convert the non-fluorescent acetoxymethyl ester of calcein into a green fluorescent form (Neri et al. 2001). Due to the absence of harmful effects on cell function, CAM can be considered a good indicator of cell viability (Weston & Parish 1992).

Propidium iodide (PI) is able to permeate compromised plasma membranes on late apoptotic cells (Kroemer et al. 1998). After crossing cellular membranes, PI intercalates with nucleic acids, showing red fluorescence. In normal live cells, PI does not cross intact plasma membranes (Vermes et al. 1995). This method is quite commonly used to evaluate the viability of cells due to its efficiency. To perform this assay, cells were seeded on 20 cm^2 dishes at a density of $5.7x10^5$ cells/dish and 24 h after seeding, cells were incubated with NEF at either 20 μM or 50 μM, for both 48h and 72 h. After the incubation periods, cells were harvested by trypsinization and centrifuged at 300xg for 3 minutes. This step was followed by incubation with CAM (final concentration: 0.1 μM) and PI (final concentration: 7.95 μM) for 15-20 minutes protected from light, at room temperature. Flow cytometry was preformed by runing 20,000 cells on a FACSCalibur flow cytometer (BD Biosciences, San Jose, California, USA) at a medium/high sample flow rate.

2.10. Caspases 3 and 9-like activities

Caspase-3 and -9-like activities were evaluated using total cellular extracts collected with the following conditions: control group, 20 μM NEF and 50 μM NEF. Similarly to the other assays, these NEF concentrations were tested for two different exposure times: 24 h and 48 h. After treatment, both floating and adherent cells were collected. Incubation media containing floating cells was centrifuged twice at 1,000xg during 5 minutes and cellular pellet was ressuspended in assay buffer (50 mM HEPES pH 7.4; 100 mM NaCl; 0.1% CHAPS; 10% glycerol; 10 mM DTT). Adherent cells were first washed with PBS 1X, a step followed by the application of 200 μl/dish of assay buffer. These cells were then harvested by scraping. Floating and adherent cells were then combined and cell lysis was performed through three cycles of freeze/thaw with liquid nitrogen/water bath and cellular extracts were then passed

through a 27G needle (20-30 strocks). Then, cellular extracts were centrifuged at 14,000xg for 5 minutes and supernatants were transfered to new eppendorfs. Protein content of each sample was determined using the Bradford assay (Bradford 1976). This method is based on interactions between the Coomassie brilliant blue G-250 dye and basic amino acids residues. The dye exists in three different forms: cationic red dye, the neutral green dye and the anionic blue dye. The latter form binds to proteins, modifying the equilibrium between the three forms and leading to a prevalence of the anionic form. This results in a change in the absorbance peak of the dye solution (Chial & Splittgerber 1993; Redmile-Gordon et al. 2013). To perform quantification protein samples were diluted and 100 µl of each sample were transfered to a 96 well. Then, 100 µl of Bradford Reagent were added to each well. Reaction was left to occur during 5-10 minutes and absorbance was read at 595 nm using SpectraMax Plus 384 Microplate Reader (Molecular Devices, Silicon Valley,CA,USA). BSA was used as a standard.

After quantification, cellular extracts containing 25 µg and 50 µg of total protein were incubated with 5 µl of a substrate solution for either caspase-3 or -9 activity (final concentration: 100 µM) for two hours at 37°C. After incubation period, absorbance was read at 405 nm SpectraMax Plus 384 Microplate Reader (Molecular Devices, Silicon Valley, CA, USA).

The method used to evaluate caspase-3 and -9 activities is based on p-nitroanilide (pNA) chromophore detection, resulting from Ac-DEVED-pNA and Ac-LEHD-pNA cleavage. This assay was calibrated with known concentrations of p-nitroaniline (pNA) and the results were expressed as % pNA released.

2.11. Statistical Analysis

Data were expressed as means ± SEM for the number of experiments indicated in the legends of the figures. Grouped comparisons were performed using two-way analysis of variance (ANOVA). Multiple comparisons were performed using one-way ANOVA followed by Bonferroni post-hoc test or Dunnet's post-hoc test. Significance was accepted with p value <0.05.

3. Results

3.1. Nefazodone effects on HepG2 cell mass

To investigate the effect of different NEF concentrations on HepG2 cells mass, we performed the SRB assay. Different concentrations of NEF were tested (0 µM, 5 µM, 10 µM, 20 µM, 50 µM and 100 µM) during different exposure times (0 h, 6 h, 24 h, 48 h and 72 h), as previously described on Section 2.3.

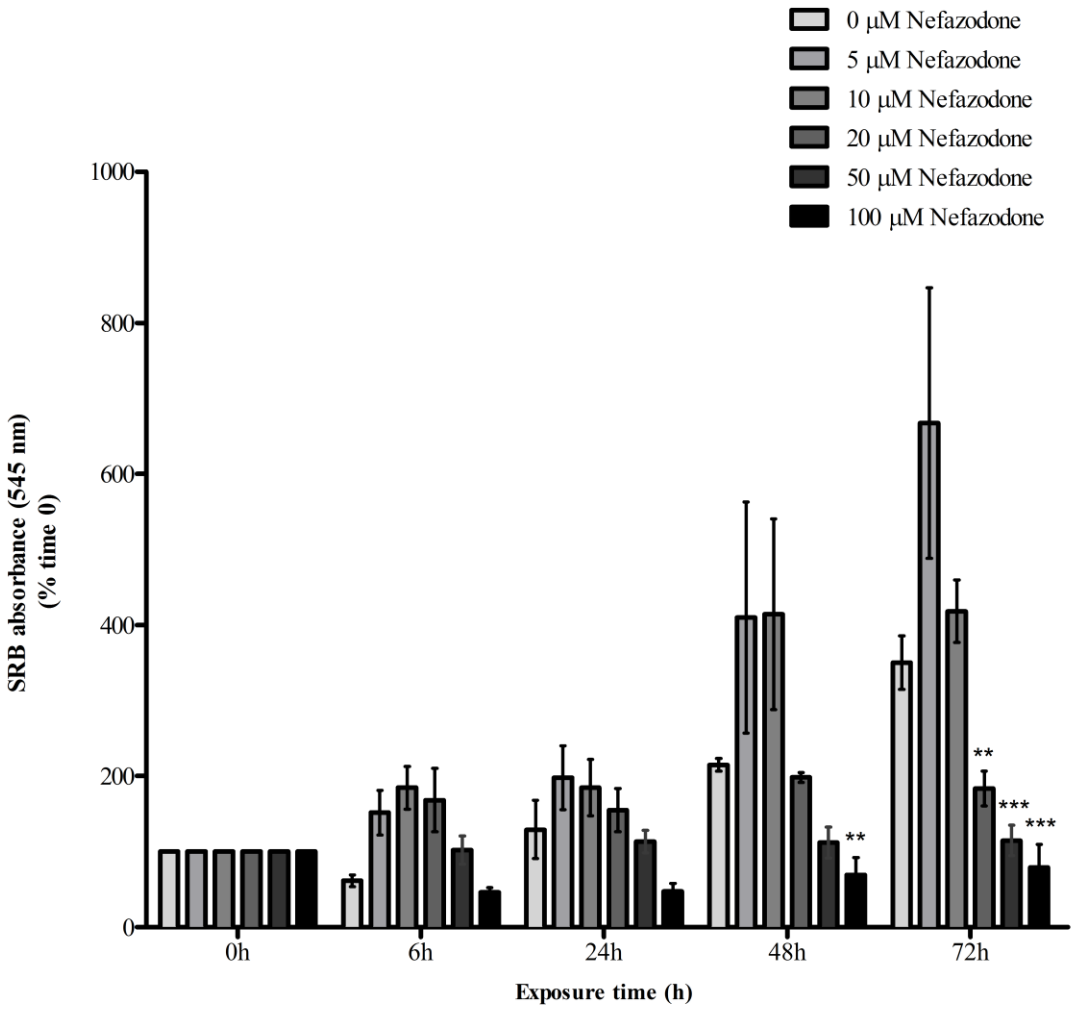

Figure 8: Effects of NEF treatment on HepG2 cell mass. Cell proliferation in the presence of different concentrations of NEF (0 µM, 5 µM, 10 µM, 20 µM, 50 µM and 100 µM) was evaluated durig different exposure times (0 h, 6 h, 24 h, 48 h and 72 h). Data show a significant decrease on cell proliferation after treatment with 100 µM for 48 h and 72 h. NEF treatment also led to a decrease in cell mass, when used in the concentrations of 20 µM and 50 µM, for 72 h. Data represent means ± SEM of five different experiments. **p<0.01 and ***p<0.001 vs control (two-way ANOVA, followed by Bonferroni post-test- comparisons to control, 0 µM).

Obtained results (Fig. 8) showed that the lowest concentrations of NEF tested (5 µM and 10 µM) had no cytotoxic effect on HepG2 cells, not compromising the increase in cell mass during the different exposure times. Actually, cells treated with 5 µM showed a higher increase on cell mass from 6 h to 72 h than cells non-treated with NEF (control group). A similar result was observed on cells treated with 10 µM NEF. However, in this experimental group, no increase in cell mass was observed between cells exposed to 10 µM NEF for 48 h and cells exposed to 10 µM NEF for 72 h. Yet, the increase on cell mass induced by both concentrations were not statistically significant, comparatively to cells in the control group. When cells were exposed to a concentration of 20 µM NEF, a significant decrease of cell mass was seen for 72 h of treatment, when compared to non-treated cells. A signifficant effect on the decrease on cell mass was also observed on cells exposed to 50 µM NEF for the same exposure time (72 h), comparatively to control cells (Fig. 8).

HepG2 cells incubated with 100 µM NEF revealed a high susceptibility to this concentration. When comparing this experimental group with non-treated cells, it is possible to verify that results revealed a tendency to a decrease on cell mass, when cells were exposed to this drug concentration. However, differences between non-treated cells and cells treated with 100 µM NEF were only statistically significant for the exposure times of 48 h and 72 h, with a reduction on cell mass under these experimental conditions (Fig. 8).

3.2. Nefazodone increases total p66Shc on HepG2 cells, but not serine 36-phosphorylated form

In order to explore possible alterations on p66Shc expression after NEF treatment, p66Shc content was evaluated through Western-Blot analysis (Fig. 9). The following experimental groups were considered: control group (non-treated cells), cells treated with 20 µM NEF and cells treated with 50 µM NEF. These conditions were applied for two time-points: 48 h and 72 h.

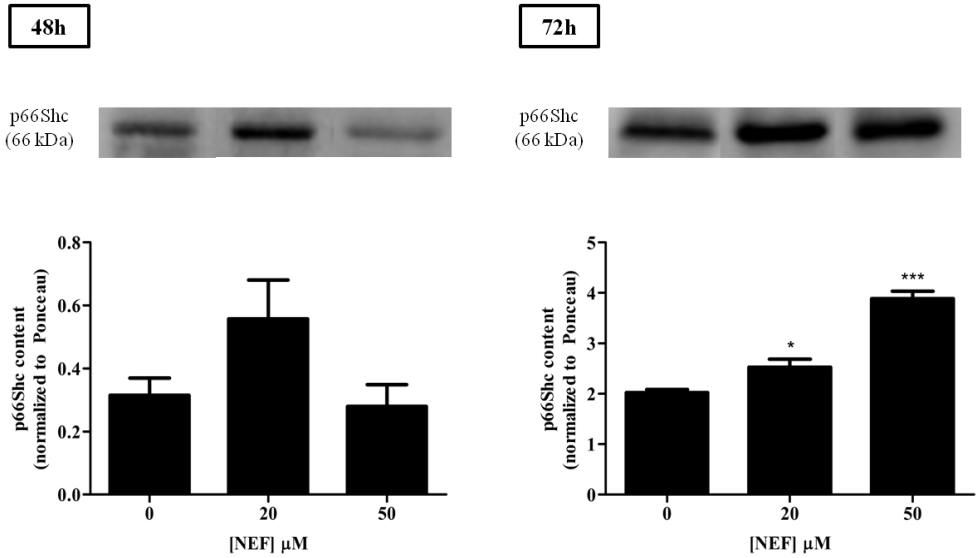

Figure 9: p66Shc content increases after NEF treatment for 72 h. p66Shc content in total cellular extracts was identified by Western Blot analysis as a protein band of 66 kDa. Cells were collected after treatment with 20 µM and 50 µM NEF for 48 h and 72 h, as described in 2.4 section. p66Shc content undergo a significant increase on cells treated with 20 µM and 50 µM NEF for 72 h, when compared to p66Shc content from non-treated cells. No significant differences were observed on p66Shc content on cells treated with the same NEF concentrations for 48 h. Ponceau labeling was used to confirm equal protein loading in each lane. Data represent means ± SEM of four different experiments. *$p<0.05$ and ***$p<0.001$ (one-way ANOVA, followed by Dunnett's post-test, comparisons to control, 0 µM). Results were normalized for Ponceau dye labeling for each lane.

No significant changes were verified regarding the total content of p66Shc from cells treated with 20 µM or 50 µM NEF for 48 h, when compared to total content of p66Shc from non-treated cells. When the exposure time was extended to 72 h, p66Shc total content significantly increased on both treatment groups, comparatively to non-treated cells. The most significant increased was verified on cells treated with 50 µM NEF. Thus, NEF treatment increases p66Shc content in HepG2 cells (Fig. 9).

Total content of serine 36-phosphorylated form was also evaluated through Western-Blotting (Fig. 10). This analysis was performed with the aim of investigating the existence of a connection between NEF administration and apoptosis triggering, through a pathway involving p66Shc activation and translocation to mitochondria. Experimental groups considered were the same from previous experiments.

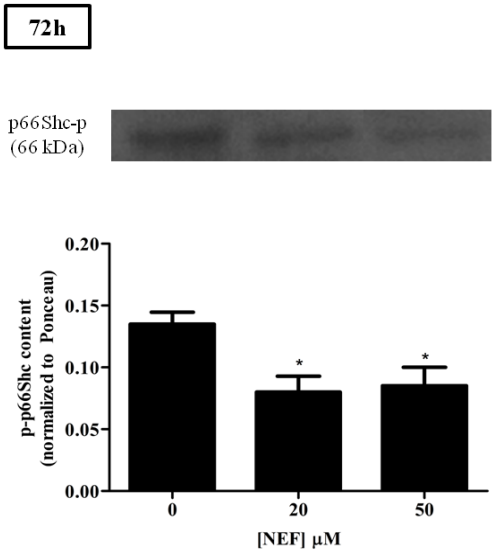

Figure 10: NEF treatment decreases serine 36-phosphorylated p66Shc (p-p66Shc) on HepG2 cells. p-p66Shc content in total cellular extracts was identified by Western-Blot as a 66 kDa band. Cells were collected after treatment with 20 µM and 50 µM NEF for 72 h, as described in 2.4. section. p-p66Shc content undergo a significant decrease on cells treated with 20 µM and 50 µM NEF for 72 h, when compared to p-p66Shc content from non-treated cells. Ponceau labeling was used to confirm equal protein loading in each lane. Data represent means ± SEM of four different experiments. *p<0.05 (one-way ANOVA, followed by Dunnett's post-test, comparisons to control, 0 µM). Results were normalized for Ponceau dye labeling for each lane.

Data from 72 h exposure to NEF showed a decrease on p66Shc phosphorylated form content. This decrease was verified for both concentrations, comparatively to cells from the control group. As mentioned above, p66Shc phosphorylated form content was also analysed on cells treated with 20 µM or 50 µM NEF for 48 h. However, the obtained results are not shown due to immunolabeling problems.

3.3. Effects of Nefazodone on nuclear morphology, mitochondrial superoxide anion and polarization

To assess alterations on nuclear morphology as well as alterations on mitochondrial membrane potential, non-treated cells and cells treated with 20 µM and 50 µM NEF were labeled with Hoechst 33342 and TMRM. These experimental conditions were performed for two treatment times: 48 h (Fig. 11) and 72 h (Fig. 12).

Confocal images revealed a decrease on cell number when comparing cells from control group with cells treated with 20 µM and 50 µM NEF during 48 h (Fig. 11). The same

effect of cell number, was also observed in cells treated with the mentioned NEF concentrations for 72 h, comparatively to cells in the control group (Fig.12).

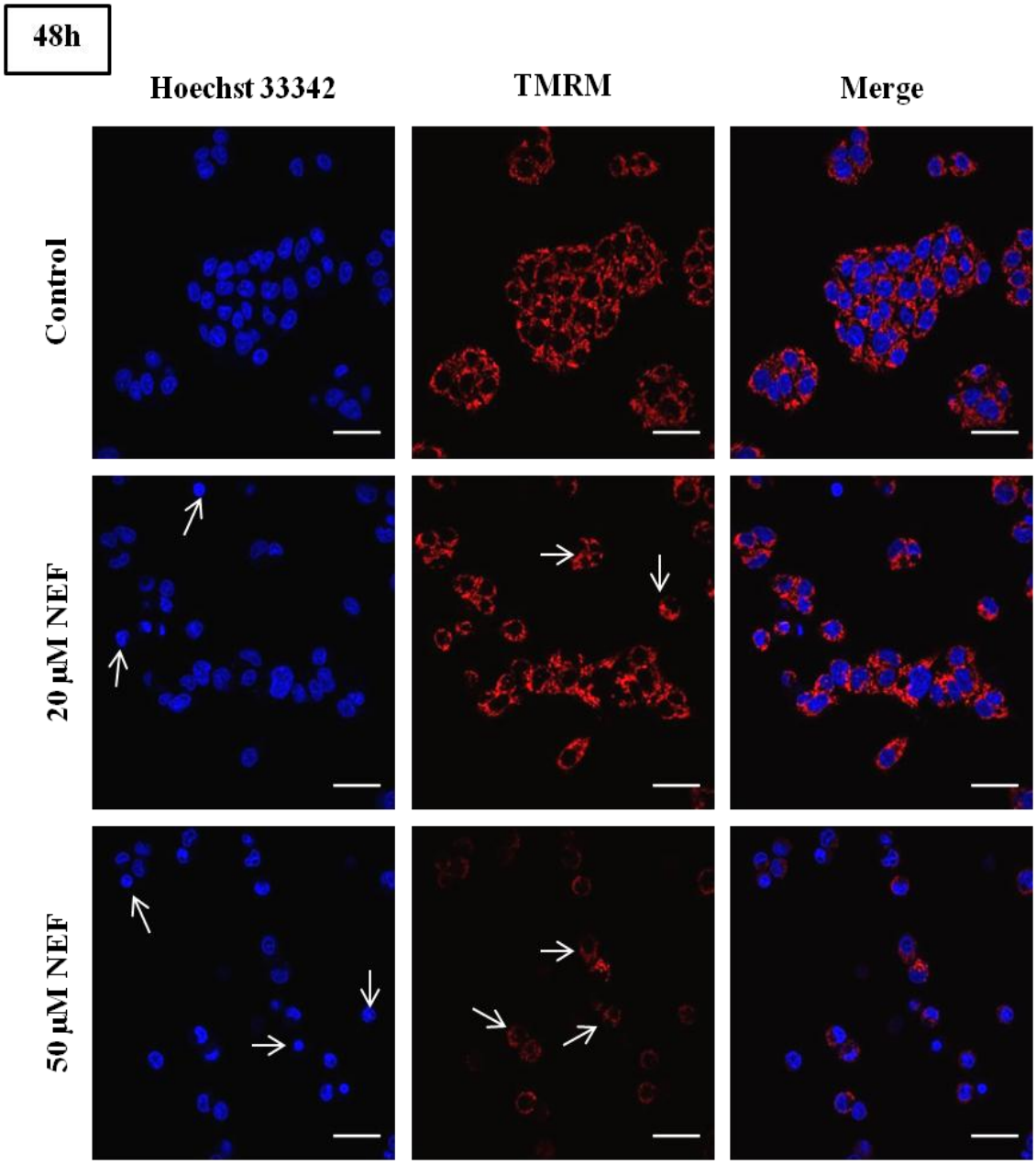

Figure 11: NEF induces alterations on HepG2 nuclear morphology and on mitochondrial membrane potential on 48 h of treatment. HepG2 cells incubated for 48 h with 20 µM and 50 µM NEF showed alterations on cell morphology. Hoechst 33342 labeling revealed a nuclear morphology characteristic of apoptosis in treated cells (20 µM and 50 µM NEF) for both treatment times. Arrows point to cells that exhibit the typical aspect of apoptotic cells. TMRM red signal was similar to control or increased slightly in some cells after treatment with 20 µM NEF, while a decrease was verified in cells treated with 50 µM NEF, suggesting that NEF treatment leads to a decrease on mitochondrial membrane potential, when tested at the highest concentration. Arrows show depolarized cells. Images were acquired by confocal microscopy using a 40x objective, scale bar = 35µm.

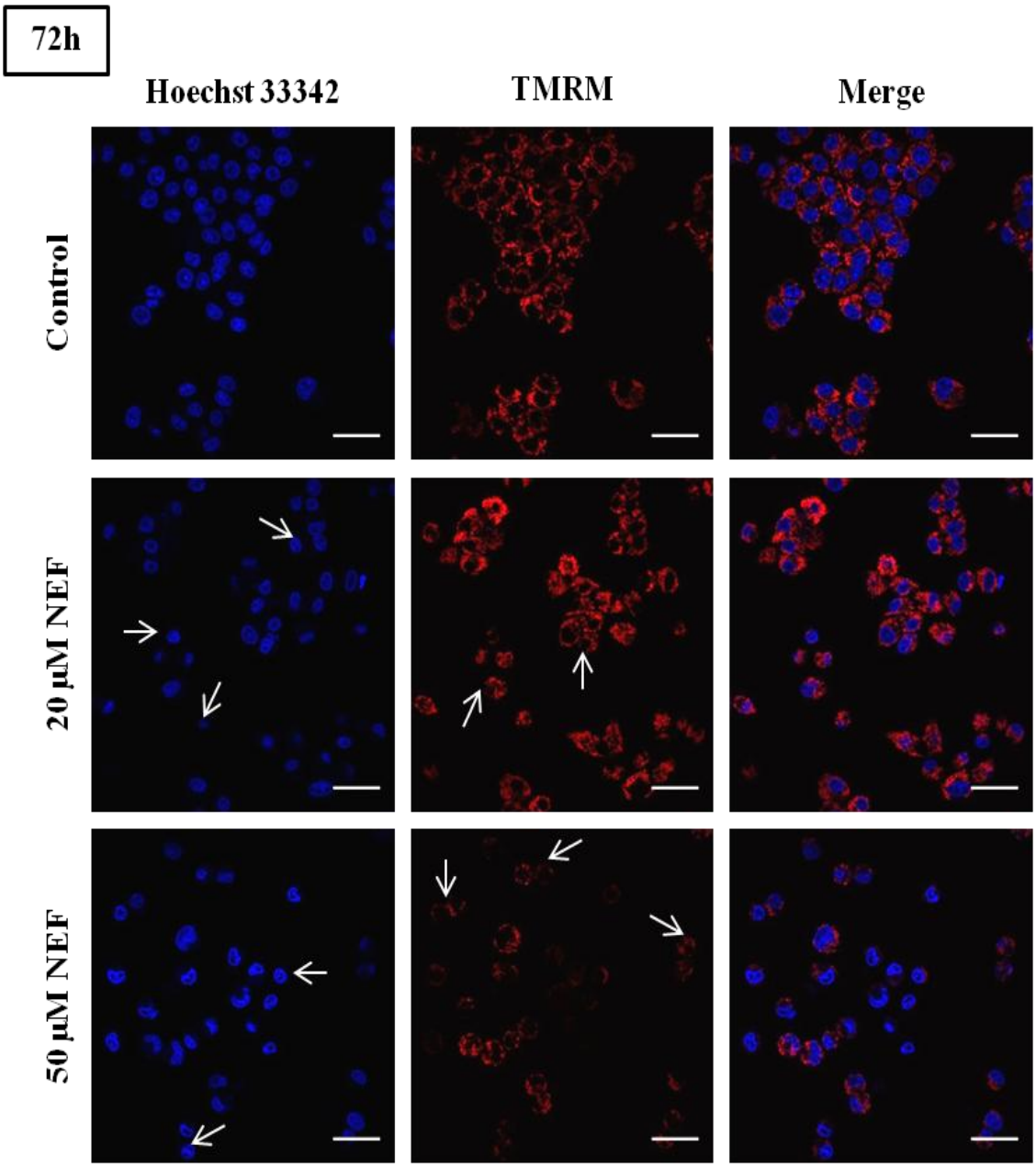

Figure 12: NEF induces alterations on HepG2 nuclear morphology and on mitochondrial membrane potential on 72 h of treatment. HepG2 cells incubated for 72 h with 20 µM and 50 µM NEF showed alterations on cell morphology. Hoechst 33342 labeling revealed a nuclear morphology characteristic of apoptosis in treated cells (20 µM and 50 µM NEF) for both treatment times. Arrows point to cells that exhibit the typical aspect of apoptotic cells.NEF treatment increased TMRM signal, at a 20 µM concentration. However, cells treated with 50 µM, showed a decrease on TMRM fluorescence, suggesting that NEF treatment, at this concentration, leads to a decrease on mitochondrial membrane potential. Arrows show depolarized cells. Images were acquired by confocal microscopy using a 40x objective, scale bar = 35µm.

Through the labbeling of cells with Hoechst 33342, alterations on nuclear shape were observed, with a loss of the typical rounded form exhibited in cells of the control group (Fig. 11 and Fig.12). Cells nucleus acquired a more irregular shape when treated with 20 μM and 50 μM NEF on the two treatment times: 48 h and 72 h. However, the more obvious changes in cell morphology and cell number were observed in cells treated with 50 μM NEF, for both incubation times. These cells exhibited profound changes in morphology, with nucleus becaming more rounded, small and similars to apoptotic cells (Fig.11 and Fig.12).

By using confocal microscopy, we also observed alterations in mitochondrial membrane potential, through the labeling with Tetramethylrhodamine, methyl ester (TMRM). The results that NEF treatment at a 20 μM concentration resulted in no changes or in small increase of TMRM fluorescence in some cells for a 48 h time-point (Fig.11), comparatively to cells in the control group. However, when NEF was applied at a 50 μM concentration for the same treatment time, a decrease on TMRM fluorescence was verified, comparatively to non-treated cells (Fig.11). So, at this concentration and time-point, NEF treatment induces a decrease on mitochondrial membrane potential, leading to cell depolarization.

When the same concentrations of NEF were used for a period of 72 h (Fig. 12), treated HepG2 cells also experienced a decrease on cell number, when compared to control cells. Comparison between non-treated cells and cells treated with 20 μM NEF showed an increase on TMRM fluorescence on cells treated with NEF, more evident than that observed on 48 h treatment time. Yet, cells treated with 50 μM NEF for 72 h exhibited low TMRM fluorescent signal, when compared to non-treated cells and cells treated with 20 μM NEF. According to this data, cells undergo an increase on mitochondrial membrane potential after NEF treatment at a 20 μM concentration while a decrease is verified when the concentration is increased to 50 μM, for the treatment time of 72 h.

To investigate NEF effect on ROS generation, cells were also labeled with MitoSOX (Fig.13 and Fig.14). This fluorescent dye is used to evaluate superoxide generation in mitochondria. In the presence of superoxide anion, this fluorescent marker is oxidized and displays red fluorescence. The experimental groups considered in this assay were the same considered for previous experiments.

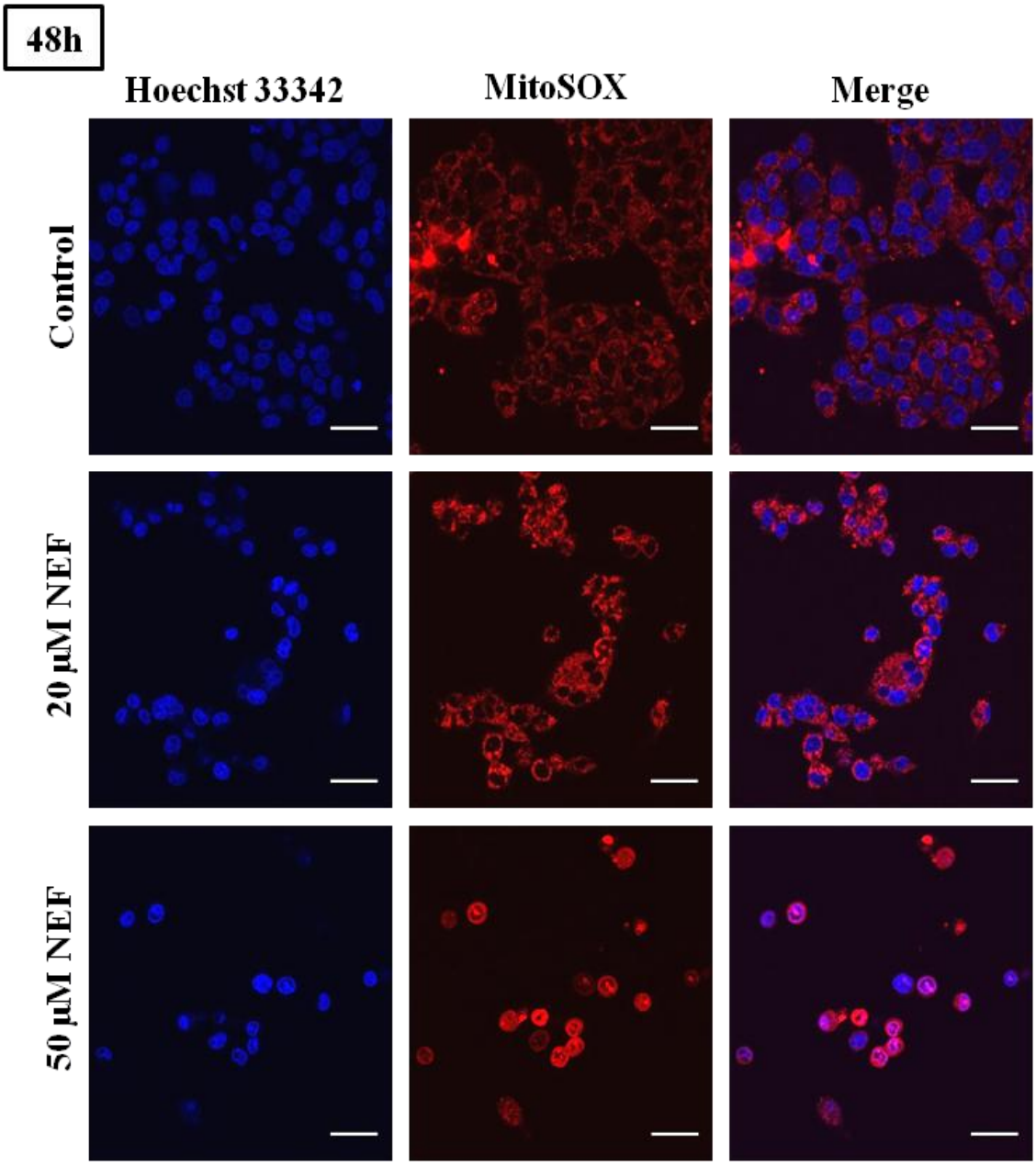

Figure 13: NEF effect on mitochondrial superoxide anion generation on 48 h of treatment. Mitochondrial superoxide anion was monitored using the red fluorescent MitoSOX red fluorescent dye. Confocal microscopy images demonstrate an increase on MitoSOX labeling, on HepG2 cells treated with 20 µM NEF, when compared to non-treated cells, on 48 h treatment time. Cells treated with 50 µM NEF undergo a severe decrease on cell number and exhibited a major MitoSOX signal, when compared to non-treated cells and cells treated with 20 µM NEF. This suggests that NEF treatment with 20 µM and 50 µM increases superoxide anion levels on HepG2 cells. Images were acquired by confocal microscopy using a 40x objective, scale bar = 35µm.

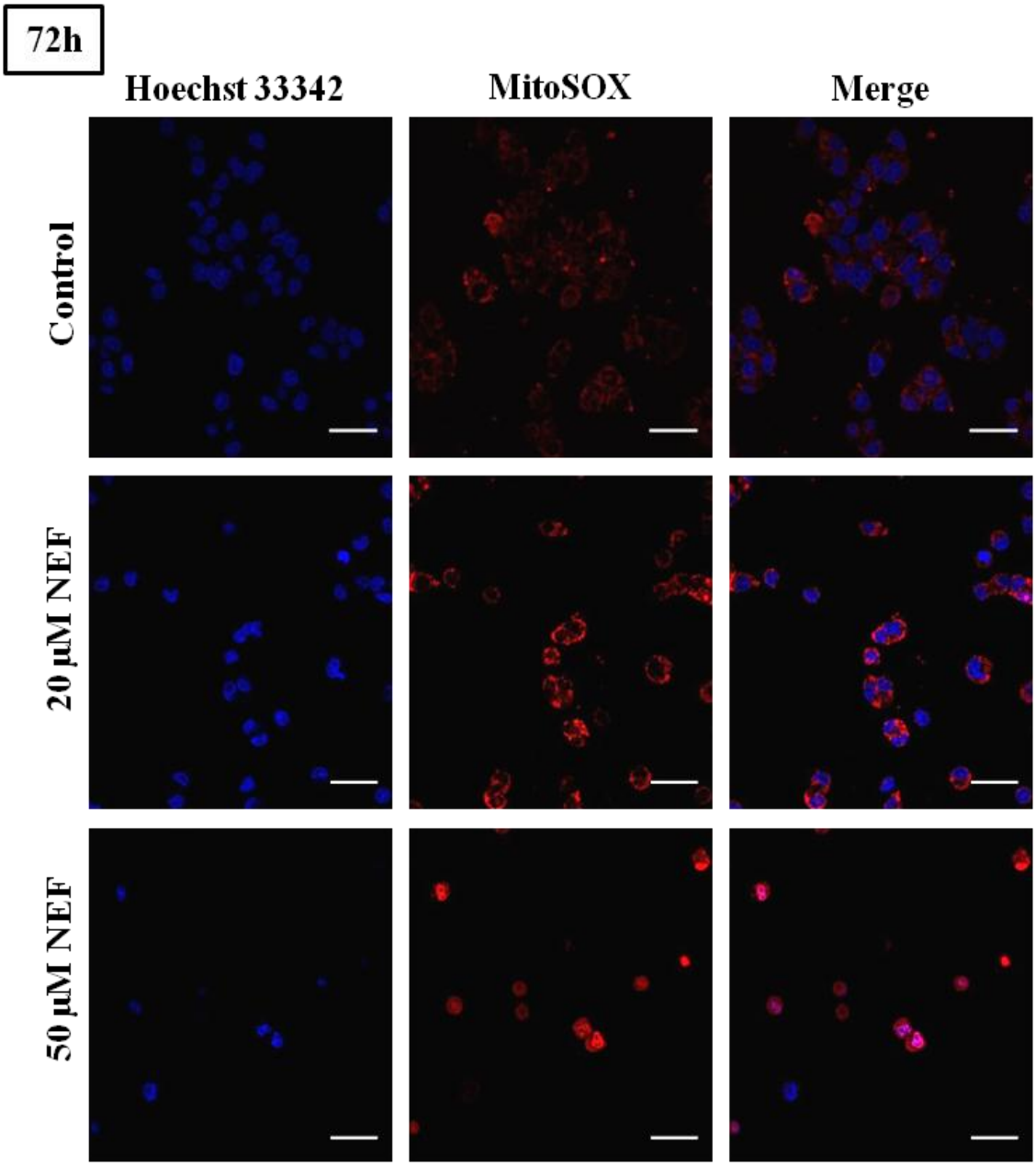

Figure 14: NEF effect on mitochondrial superoxide anion generation on 72 h of treatment. Mitochondrial superoxide anion was monitored using the red fluorescent MitoSOX red fluorescent dye. Confocal microscopy images demonstrate an increase on MitoSOX labeling, on HepG2 cells treated with 20 µM NEF, when compared to non-treated cells, on 72 h treatment time. Cells treated with 50 µM NEF undergo a severe decrease on cell number and exhibited a major MitoSOX signal, when compared to non-treated cells and cells treated with 20 µM NEF. This suggests that NEF treatment with 20 µM and 50 µM increases superoxide anion levels on HepG2 cells. Images were acquired by confocal microscopy using a 40x objective, scale bar = 35µm.

The treatment of HepG2 cells with 20 µM and 50 µM NEF decreased cell number, in comparison to non-treated cells. This decrease in cell number was more obvious on cells treated with 50 µM NEF, for both exposure times (48 h and 72 h).

On cells treated with 20 µM during a period of 48 h, was possible to verify an increase on MitoSOX signal, when compared to non-treated cells. This increase on MitoSOX red fluorescence, suggests an increase on superoxide anion levels on cells exposed to this experimental condition, when compared to non-treated cells. When cells were treated with 50 µM NEF, an increase on MitoSOX signal was also verified, comparatively to cells in the control group. MitoSOX labeling in this cells was also higher than MitoSOX labeling in cells treated with 20 µM NEF (Fig.13). According to this data, superoxide anion content were higher in NEF vs. the control group.

When the same concentrations of NEF (20 µM and 50 µM) were used on HepG2 cells for a 72 h period, the data also showed a decrease on cell number in the treated group, when compared to non-treated cells. Cells treated with 20 µM NEF presented an increase on labeling with MitoSOX fluorescent dye, compared to cells in the control group (Fig.14).

In cells treated with 50 µM NEF for 72 h (Fig.14), a more intense labeling with MitoSOX was also observed, comparatively to cells in the control group. As demonstrated in the data obtained from the treatment time of 48 h, data from 72h exposure to 20 µM and 50 µM NEF also suggest that NEF induces superoxide anion production on mitochondria.

3.4. Nefazodone induces alterations on mitochondrial membrane potential

In order to investigate the effect of NEF on mitochondrial function, alterations on ΔΨm were also evaluated again by using TMRM. As previously mentioned, TMRM is a positively charged fluorescent dye, accumulated by functional mitochondria. So, higher TMRM fluorescence indicate higher mitochondrial membrane potential. So, mitochondrial membrane potential was also evaluated in all experimental groups through flow cytometry, using TMRM (Fig.15).

After 48h of exposure to NEF, cells treated with 20 µM showed a significant increase on TMRM fluorescence, when compared to cells in the control group. This result suggests an increase on the ΔΨm on this experimental group. For the same treatment time, cells treated

with 50 µM NEF showed no significant alterations regarding TMRM fluorescence, when compared to control cells.

On cells exposed for 72 h to NEF, no significant differences were verified on TMRM fluorescence between cells of the control group and cells treated with 20 µM NEF. However, cells treated with 50 µM for 72 h, revealed a significant increase on TMRM fluorescence, comparatively to non-treated cells. As observed on cells treated with 20 µM NEF for 48 h, cells treated with 50 µM NEF for 72 h also revealed an increase on mitochondrial membrane potential, after treatment.

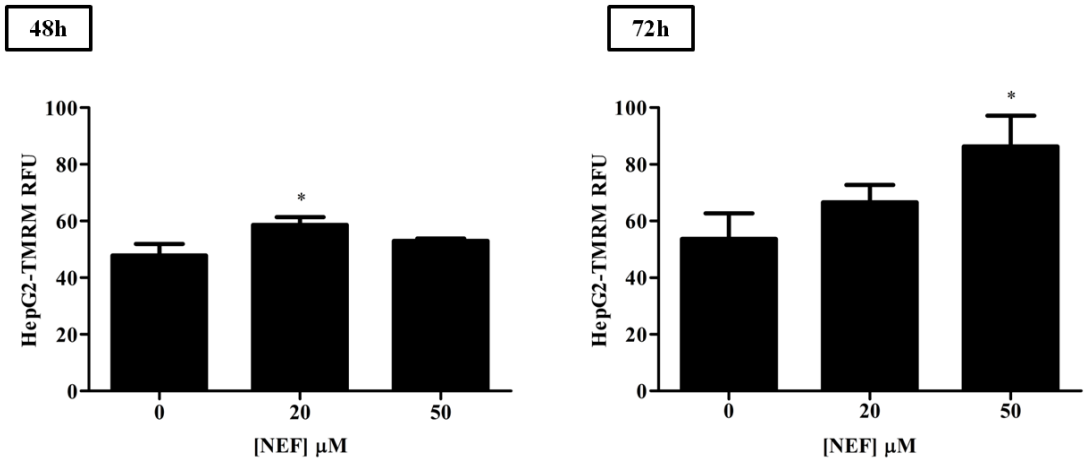

Figure 15: Mitochondrial membrane potential alterations upon NEF treatment. Mitochondrial membrane potential alterations were evaluated using TMRM and analyzed through flow cytometry. Cells treated with 20 µM NEF for an incubation time of 48 h, showed an increase of TMRM fluorescence, indicating an increase on ΔΨm. For the exposure time of 72 h, only cells treated with 50 µM NEF showed differences of TMRM fluorescence, when compared to control group. These cells exhibited an increase of TMRM fluorescence, suggesting also an increase on mitochondrial membrane potential. Results were expressed as relative units of fluorescence (RFU). Data represent mean ±SEM of six different experiments. *$p<0.05$ (one-way ANOVA, followed by Dunnett's post-test, comparisons to control, 0 µM).

3.5. Evaluation of cell viability after NEF treatment through flow cytometry

To evaluate cell viability on HepG2 cells treated with 20 µM and 50 µM NEF for 48 h and 72 h, flow cytometry was combined with the use of fluorescent dyes Calcein-AM (CAM) and Propidium Iodide (PI). The former marker is converted into a green fluorescent form by active intracellullar esterases while PI crosses damaged plasma membranes from necrotic cells and intercalates with nucleic acids, displaying red fluorescence. Thus, the combination

of the two markers allowed to evaluate the occurrence of apoptosis vs. necrosis on cells treated with NEF (Fig.16-A;B and Fig.17-A;B).

Three quadrants were considered for data analysis: dead cells were detected on quadrant 1 (Q1-CAM negative/PI positive), while live cells were detected on quadrant 4 (Q4-CAM positive/PI negative). Quadrant 2 (Q2-CAM positive/PI positive) comprises permeabilized cells, with a plasmatic membrane already damaged, allowing PI crossing. Cells on quadrant 3 (Q3-CAM negative/PI negative), cell debris, were excluded from this analysis (Fig.14-A).

After 48h of exposure to NEF, no significant differences were observed in the dead cells population (CAM negative/PI positive fluorescence, Q1) between cells from control group, cells treated with 20 µM NEF and cells treated with 50 µM NEF. Cells treated with 20 µM NEF, showed no significant changes on permeabilized cells population comparatively to non-treated cells. However, the exposure for 48 h to a concentration of 50 µM NEF increased permeabilized cells population, not only in comparison to non-treated cells, but also in comparison to cells treated with 20 µM NEF (Fig.16-B). Live cells population also underwent changes after NEF exposure: treatment with 50 µM NEF for 48 h led to a decrease of live cells population, when compared to non-treated cells. The decrease on live cells population after treatment with 50 µM NEF was also statistically significant when compared to live cells treated with 20 µM NEF (Fig.16-B). The concentration of 20 µM NEF caused no changes on live cells population when compared to live cells population from the control group.

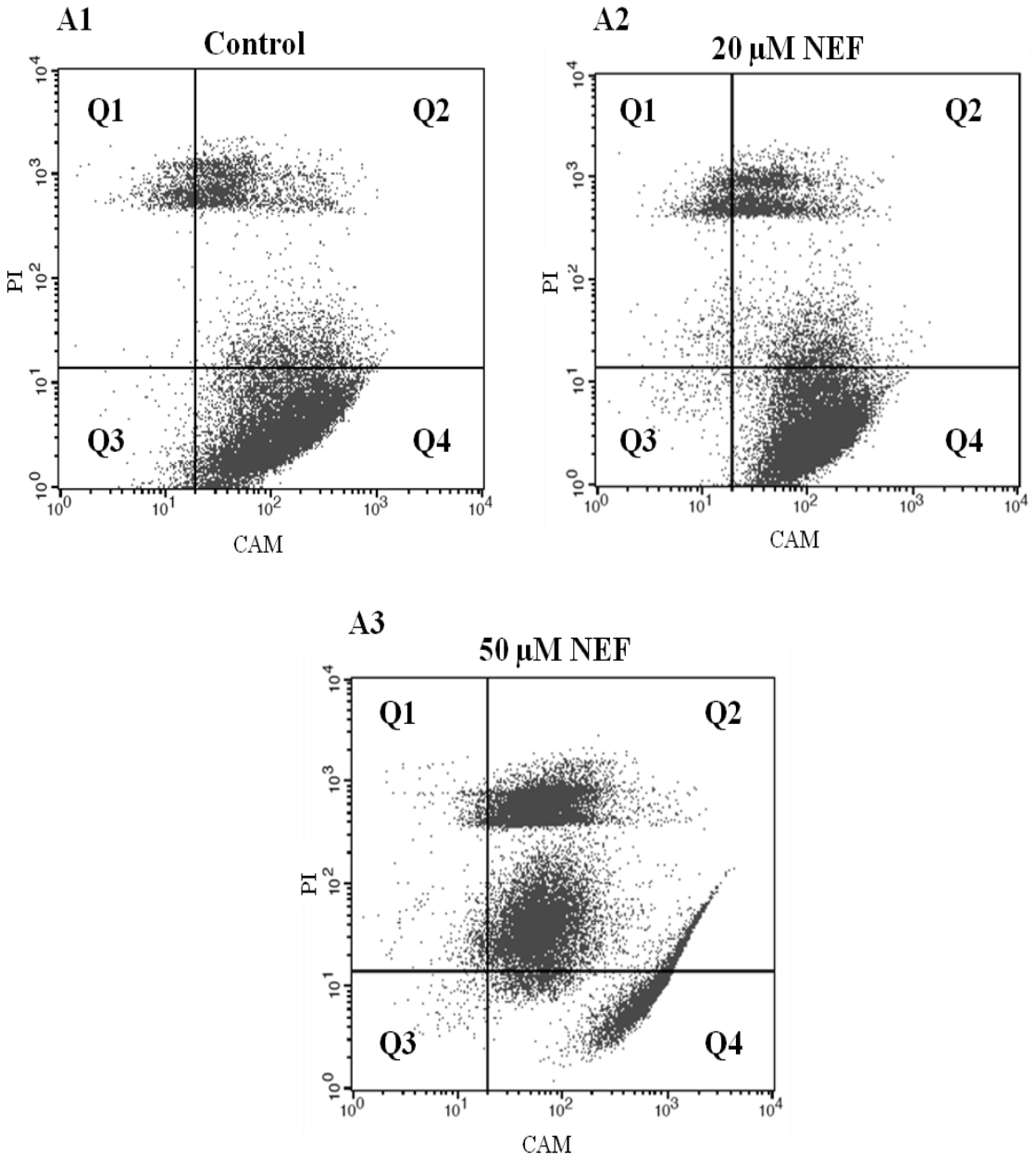

Figura 16 (A): Representative flow cytometry results for HepG2 cells exposed to 20 µM and 50 µM NEF for 48 h. The abscissa and ordinate represent the fluorescence intensity of Calcein AM (CAM) and propidium iodide (PI), respectively.

Q1-calcein negative/PI positive (CAM^-/PI^+), dead cells
Q2-calcein positive/PI positive (CAM^+/PI^+), permeabilized cells
Q3- calcein negative/PI negative (CAM^-/PI^-), cell debris (quadrant not considered in the data analysis).
Q4-calcein positive/PI negative (CAM^+/PI^-), live cells.

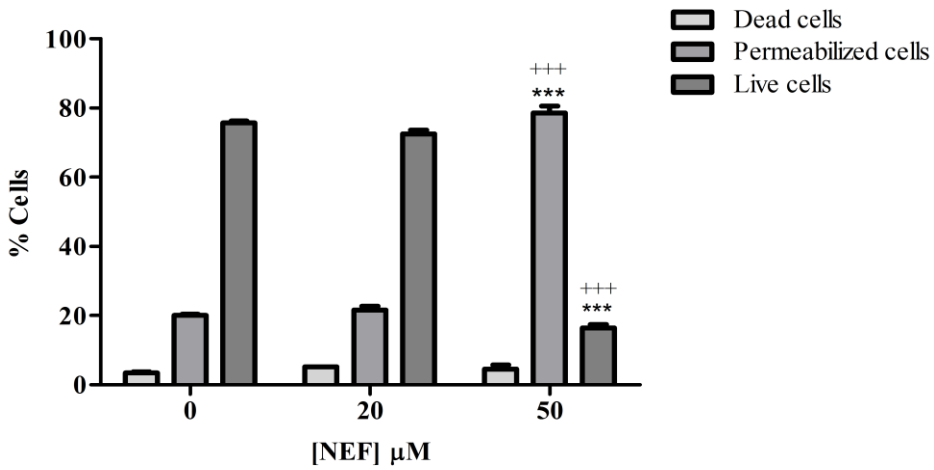

Figure 16 (B): Quantitative analysis of NEF-induced cell death on HepG2 cells, after 48 h treatment with NEF. The effect of NEF on cell death was evaluated through flow cytometry, using the combination of CAM and PI fluorescent dyes. Results showed that NEF, at a concentration of 50 µM, leads to an increase on permeabilized cells population, comparatively to non-treated cells and cells treated with 20 µM NEF. Nefazodone, at a concentration of 50 µM , also caused a significant decrease on live cells population, after 48 h treatment, comparatively to non-treated cells and cells treated with 20 µM NEF. Data represent mean ± SEM of dead cells (CAM negative/PI positive), permeabilized cells (CAM positive/PI positive) and live cells (CAM positive/PI negative), for six different experiments. ***$p<0.001$ - control vs 50 µM of NEF and $^{+++}p<0.001$- 20 µM vs 50 µM NEF (one-way ANOVA, followed by Bonferroni post-test).

When the treatment time with NEF was expanded to 72 h, cells treated with 50 µM showed a decrease on dead cells percentage, when compared to percentage of dead cells in the control group (Fig.17-B). Furthermore, no significant differences were measured between dead cells in the control and dead cells found when treating with 20 µM NEF. The analysis of permeabilized cells population showed differences between cells in the control group and cells treated with 50 µM NEF, with an increase on permeabilized cells population after treatment with 50 µM NEF for 72 h, comparatively to permeabilized cells population in the control group. This increase in permeabilized cells after treatment with 50 µM NEF was also statistically significant, when compared to permeabilized cells population after 20 µM NEF. Live cells population also underwent changes after NEF treatment: cells treated with 50 µM NEF for 72 h, underwent a significant decrease on live cells, when compared to live cells from control group (Fig.17-B). The same NEF concentration also led to a reduction on live cells population, relatively to live cells population on cells treated with 20 µM NEF. The treatment with 20 µM NEF, did not change live cells population, relatively to live cells population in the control group.

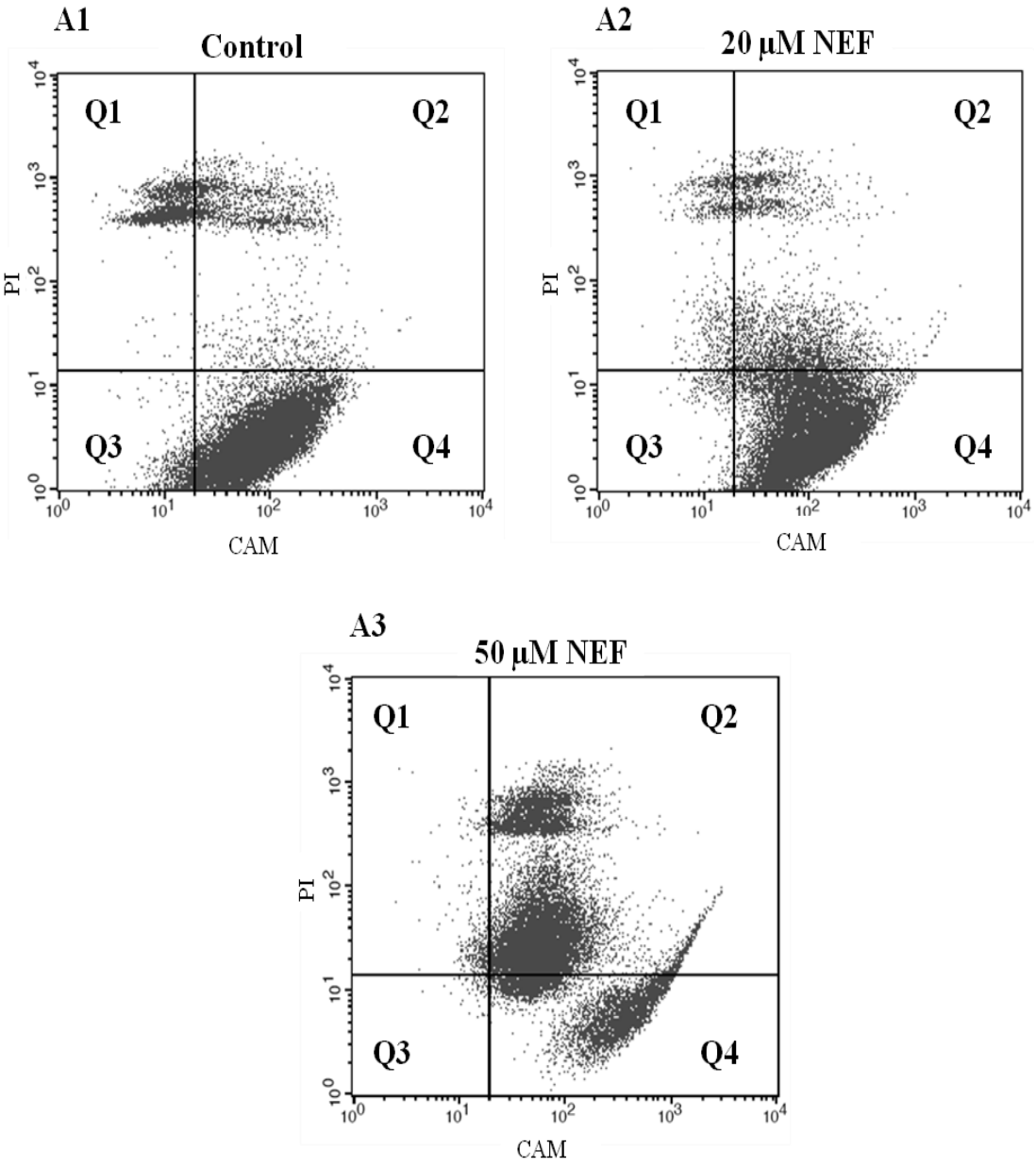

Figure 17 (A): Representative flow cytometry results for HepG2 cells exposed to 20 µM and 50 µM NEF for 72 h . The abscissa and ordinate represent the fluorescence intensity of Calceim-AM (CAM) and propidium iodide (PI), respectively.

Q1-calcein negative/PI positive (CAM^-/PI^+), dead cells
Q2-calcein positive/PI positive (CAM^+/PI^+), permeabilized cells.
Q3- calcein negative/PI negative (CAM^-/PI^-), cell debris (quadrant not considered in the data analysis).
Q4-calcein positive/PI negative (CAM^+/PI^-), live cells.
.

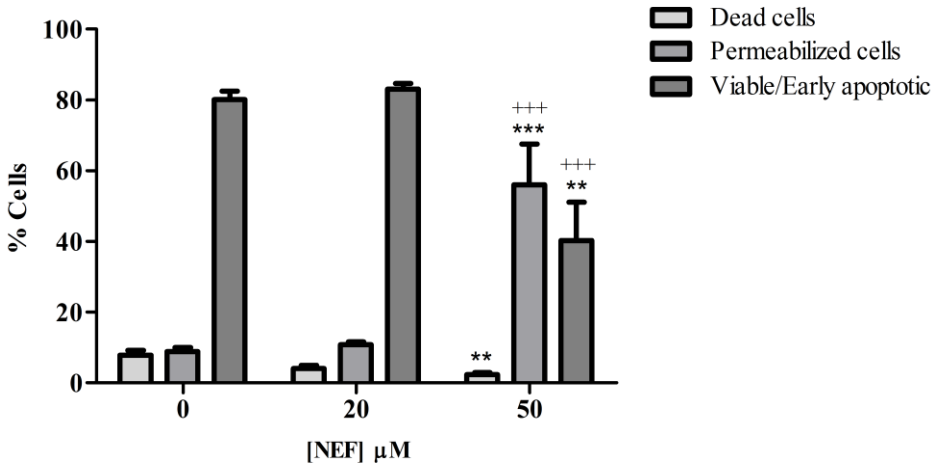

Figure 17 (B): Quantitative analysis of NEF-induced cell death on HepG2 cells, after 72 h treatment with NEF. The effect of NEF on cell death was evaluated through flow cytometry, using the combination of CAM and PI probes. Results showed that NEF, at a concentration of 50 µM, led to a significant decrease on dead cells population, comparatively to non-treated cells. The same concentration of NEF also led to significant alterations on permeabilized cells population and live cells population. Permeabilized cells population underwent an increase after treatment with 50 µM NEF, comparatively to cells in the control group and cells treated with 20 µM NEF. Live cells underwent a decrease after treatment with 50 µM NEF, comparatively to live cells in the control group and after treatment with 20 µM NEF. Data represent mean ± SEM of dead cells (CAM negative/PI positive), permeabilized cells (CAM positive/PI positive) and live cells (CAM positive/PI negative), for six different experiments.**p<0.01- control vs 50 µM NEF ***p<0.001 - control vs 50 µM NEF, $^{+++}$p<0.001- 20 µM vs 50 µM NEF (one-way ANOVA, followed by Bonferroni post-test).

3.6. Effect of Nefazodone on caspase-3 and -9-like activities

The caspase-3 and -9-like activities in cells incubated with 20 µM and 50 µM NEF for 24 h and 48 h were evaluated following the cleavage of the colorimetric substrates Ac-DEVD-pNA and Ac-LEHD-pNA, respectively.

Cells treated with 20 µM or 50 µM NEF for 24 h, revealed no significant differences in caspase-3-like activity, comparatively to cells in control group (Fig.18). On the other hand, caspase-9-like activity increased, after 20 µM NEF treatment (Fig.18). This increase was statistically significant, when compared to caspase-9-like activity on non-treated cells. No significant differences were verified on caspase-9-like activity on cells exposed to a higher NEF concentration (50 µM), for the same time-point.

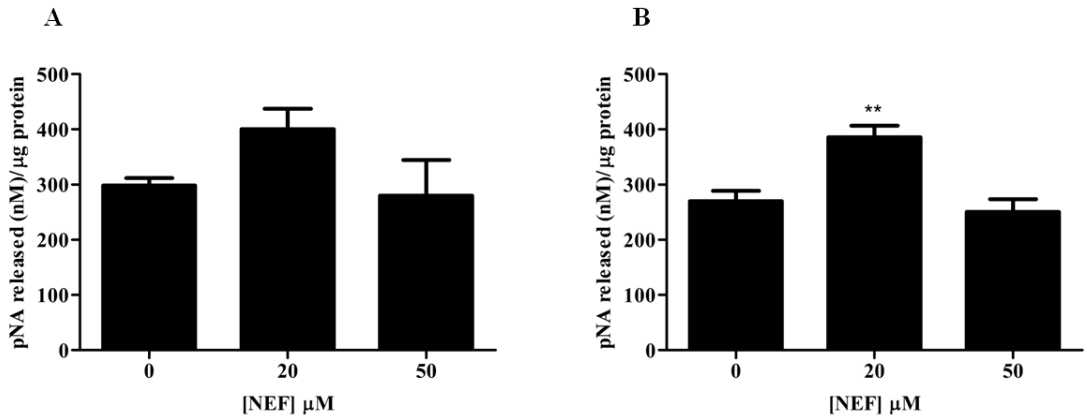

Figure 18: Effect of exposure to NEF for 24 h on caspase-3 and -9 like activities. The activities of effector caspase-3 (A) and initiator caspase-9 (B) were evaluated 24h after cells treatment with 20 µM and 50 µM NEF, as described on section 2.10. Results were expresssed as concentration of pNA released per µg protein and calibration was done using known concentrations of pNA. No differences were observed for caspase-3-like activity between cells on control group and cells treated with 20 µM or 50 µM NEF. Cells treated with 20 µM NEF showed an increase on caspase-9-like activity, comparatively to non-treated cells. No differences were found on caspase-9-like activity after treatment with 50 µM NEF. Data represent mean ±SEM of three different experiments. Data represent mean ±SEM of four different experiments. **p<0.01 (one-way ANOVA, followed by Dunnett's post-test, comparisons to control, 0 µM).

When the same concentrations of NEF (20 µM and 50 µM) were tested for 48 h treatment, cells treated with 20 µM NEF, underwent a significant increase on caspase-3-like activity (Fig.19), when compared to cells in the control group. Caspase-3-like activity on cells treated with 50 µM NEF during the same period was also significantly higher, when compared to cells in the control group. Despite the two concentrations led to an increase on caspase-3-like activity, the most significant increase was verified on cells treated with 20 µM NEF (Fig.19).

Caspase-9-like activity in cells treated for 48 h with 20 µM NEF increased, suggesting that cells underwent apoptosis under these conditions (Fig.19). Caspase-9-like activity did not change significantly in cells treated with 50 µM NEF for the same period of time, comparatively to the control.

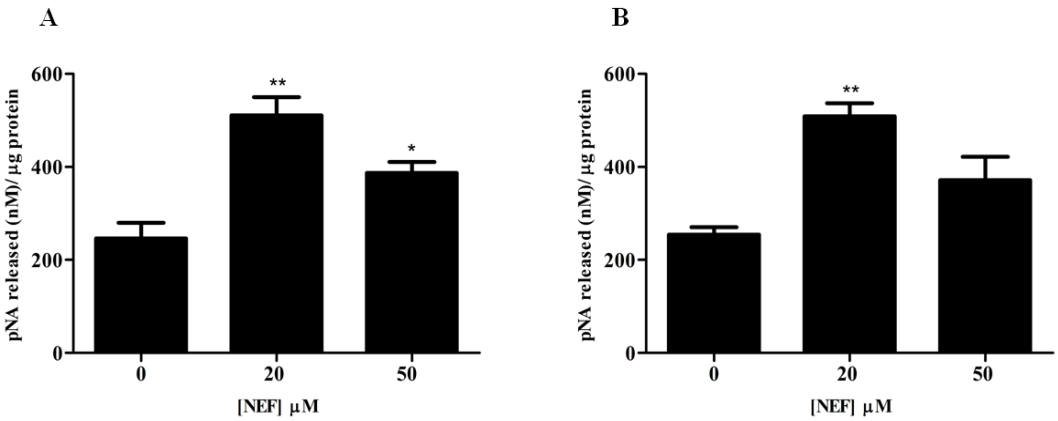

Figure 19: Effect of exposure to NEF for 48 h on caspase-3 and -9-like activities. The activities of effector caspase-3 (A) and initiator caspase-9 (B) were evaluated 48h after cells treatment with 20 µM and 50 µM NEF, as described on section 2.10. Results were expresssed as concentration of pNA released per µg protein and calibration was done using known concentrations of pNA. Treatment with 20 µM of NEF for 48 h increased caspases-3 and -9-like activities on HepG2 cells. However, treatment with 50 µM NEF only increased caspase-3-like activity, while no changes were observed on caspase-9 -like activity under the same treatment. Data represent mean ± SEM of three different experiments. *$p<0.05$ and **$p<0.01$ (one-way ANOVA, followed by Dunnett's post-test, comparisons to control, 0 µM).

4. Discussion

Nefazodone is an antidepressive agent developed by Bristol-Myers Squibb and widely used in the treatment of depression. However, this drug was withdrawn from the market due to the emergence of several reports of liver injury and failure in patients treated with NEF (Aranda-Michel et al. 1999). The effect of NEF on mitochondrial function impairment was already described by other authors suggesting that NEF interferes on normal OXPHOS complexes activity (Nadanaciva et al. 2007; Dykens et al. 2008). Nefazodone also increases ROS levels and decreases antioxidant defenses (Dykens et al. 2008).

Taking this data into consideration, our hypothesis states that a link exists between NEF administration and apoptosis induction, through a pathway involving p66Shc activation and subsequent translocation to mitochondria. According to previous works, this pathway is triggered in a cell stressful condition such as oxidative stress. Although the concentrations here used (20 µM and 50 µM) are higher than those found in the plasma of treated patients patients, we wanted to test an acute treatment protocol at a higher dosage to uncover biological effects.

As mentioned above, p66Shc signalling pathway is triggered in a cell stressful condition, that leads to PKC-β activation, involved on p66Shc phosphorylation on serine 36. Phosphorylated p66Shc is recognized by Pin1 that catalyzes its cis-trans isomeration. At this point, PP2A dephosphorylates p66Shc, allowing its entry into mitochondria. Once in mitochondria, p66Shc binds to cyt c and can act as an oxidoreductase, shuttling electrons from cyt c to molecular oxygen and leading to an increase on ROS generation (Raffaello & Rizzuto 2011).

To explore this hypothesis, we first performed an SRB assay, to evaluate the cytotoxic effect of NEF, when applied on different concentrations and during different treatment times. This SRB assay (Fig. 8) was performed to choose two NEF concentrations and two treatment times to perform subsequent assays described on materials and methods section. Surprisingly, results showed that cells treated with the lowest concentrations of NEF (5 µM and 10 µM) showed a non-significant increase of cell mass compared with control cells. When NEF concentration was increased to 20 µM and 50 µM and applied for 72 h, cell mass undergo a signicant decrease, verified through the decrease on SRB absorbance. A significant decrease on cell mass was also observed on cells exposed to 100 µM for 48 h and 72 h. Nevertheless,

the decrease verified after treatment with 100 µM was so severe, that led to the exclusion of this concentration from our work. Thus, we avoid the possibility of cells not being in sufficient number to perform the other assays described on the present work. The loss of cell mass after NEF treatment, as detected by the SRB technique may result both from cell death or from the inhibition of cell cycle.

Attending to this data, the two concentrations of 20 µM and 50 µM NEF were chosen to perform further assays in this work. We tested the mentioned concentrations for 48 h and 72 h time-points on the following assays: western-blot analysis, confocal microscopy, flow cytometry using TMRM labeling and flow cytometry using CAM and PI labeling.

As stated above, our initial hypothesis proposes that NEF treatment leads to apoptosis on HepG2 cells through a pathway involving p66Shc activation and translocation to mitochondria. In order to confirm p66Shc activation and phosphorylation, p66Shc and p66Shc phosphorylated content were analysed by Western-Blotting on cells treated with 20 µM and 50 µM NEF for 48 h and 72 h.

No differences were observed on p66Shc total content after NEF treatment, for the 48h time-point (Fig.9). This data suggest that, at this time point and concentrations, p66Shc total protein is unchanged. However, when the same conditions were tested for a longer period (72 h), p66Shc total content increased significantly on cells treated with NEF at 20 µM or 50 µM concentrations (Fig.9). These results support a p66Shc activation induced by NEF treatment. However, to confirm this hypothesis, total content of phosphorylated p66Shc was also evaluated. Despite the p66Shc increase verified on cells treated with 20 µM or 50 µM NEF for 72 h, a different result was obtained when the content of p66Shc phosphorylated form was analysed through Western-Blotting. After 72 h of NEF exposure, phosphorylated p66Shc content significantly decreased (Fig.10). Despite the increase on p66Shc content seems consistent with the activation of this protein by PKC-β, more experiments should be performed in order to evaluate alterations on p66Shc phosphorylated form. A fast p66Shc phosphorylation/dephosphorylation cycle may also occur after NEF treatment, which ultimately will cause a lower detectable amount of p66Shc. Thus, although the connection between NEF administration and p66Shc phosphorylation remains unclear, our work found evidences that support that NEF increases ROS levels and apoptosis triggering.

Confocal microscopy images showed that NEF treatment, on both concentrations (20 µM and 50 µM) and for both treatment times (48h and 72h) led to alterations on HepG2 cell

number and nuclear morphology (Fig.11 and Fig.12). The treatment with both concentrations for both time points, significantly decreased cell number, comparatively to non-treated cells. The decrease on cell number verified through confocal microscopy after NEF treatment at 20 µM and 50 µM concentrations for 72 h of treatment, is consistent with the results obtained in the SRB assay, where these concentrations also led to a significant decrease on cell mass, when compared to control cells. Despite the SRB assay was not as efficient in detecting a significant reduction on cell mass upon NEF treatment at the same concentrations for 48 h of exposure, confocal microscopy confirmed that at the mentioned concentrations and exposure time, the reduction on cell number is already evident, especially in cells treated with NEF at a 50 µM concentration (Fig.11 and Fig.12). This decrease in cell number verified for both concentrations and time-points is consistent with data provided by other works, where the decrease on cell number after NEF treatment was also reported (Dykens et al. 2008).

Regarding cell morphology, cells nucleus labeled with Hoechst 33342 after NEF treatment appeared smaller (Fig.11 and Fig.12). This feature, combined with the dense appearance of cells treated with NEF suggest that these cells undergo pyknosis, one of the main characteristics of cells under apoptotic process and resulting from chromatin condensation (Kerr et al. 1972; Elmore 2007). These alterations were more obvious in the few cells that survived treatment with 50 µM NEF for 48 h and 72 h.

Despite the link between NEF administration and p66Shc activation and translocation to mitochondria is still missing, we found some evidences supporting a connection between NEF administration, ROS generation and cell death.

The labeling of treated cells with MitoSOX red fluorescent dye and subsequent visualization under confocal microscopy, revealed that NEF treatment increases ROS levels (Fig.13 and Fig.14). Cells incubated with 20 µM and 50 µM NEF for 48 h and 72 h showed an increase in MitoSOX fluorescence, when compared to control cells. Thus, this data suggest that superoxide anion levels are higher on cells treated with NEF, comparatively to non-treated cells. This information is consistent with data provided on other assays, when NEF administration led to increased ROS levels (Dykens et al. 2008). This increase on ROS levels could be due to p66Shc effects on mitochondria (Giorgio et al. 2005). Besides being consistent with previous data, this increase on ROS levels, combined with the decrease on cells mass verified on SRB assay and confocal microscopy supports the idea that NEF may induce cell death through a mechanism that involves ROS generation.

Besides the data related with ROS levels, confocal microscopy also provided other informations to reinforce the idea of NEF interferes with a normal hepatocyte function. Confocal microscopy images from cells labeled with TMRM revealed that treatment with 20 μM NEF for 48 h and 72 h (Fig.11 and Fig.12) appear to suggest a small increase in the accumulation of this marker, comparatively to non treated cells and cells treated with 50 μM NEF. Since TMRM is positively-charged, this fluorescent dye would be more accumulated in polarized mitochondria (negative inside). Thus, the increase on TMRM fluorescence suggests an increase on mitochondrial membrane potential. This fact can be related with the capacity of NEF to inhibit complex V of respiratory chain, leading to a transitional increase on mitochondrial membrane potential (Nadanaciva et al. 2007). This increase on mitochondrial membrane potential can also be related with the triggering of the apoptotic process, as already reported by several authors (Banki et. al 1999). However, the highest concentration of NEF (50 μM) led to a decrease on mitochondrial membrane potential, on both time points (Fig.11 and Fig.12). This effect may be due to the marked cytotoxic effect of this concentration over HepG2 cells, leading to the inhibition of other respiratory chain complexes, such complex I and complex IV, and consequently inducing cell depolarization. The ability of NEF to compromise OXPHOS was already verified when NEF was tested at a 50 μM concentration in experiments using bovine heart mitochondria (Nadanaciva et al. 2007). Thus, data provided by confocal microscopy are consistent with previous published works indicating that NEF administration induces ROS generation and alterations on mitochondrial membrane potential, with an occurrence of cell depolarization at the highest NEF concentration (Nadanaciva, Bernal, et al. 2007; Dykens et al. 2008).

Once more, this data corroborate the decrease on cell mass and changes on cell nucleus morphology verified after NEF treatment, typically seen in apoptotic cells. Data still support the role of NEF treatment on cell death triggering. To confirm the obtained results, mitochondrial membrane potential was also evaluated through flow cytometry using, once more, TMRM labeling (Fig.15). Results showed that NEF administration at a concentration of 20 μM for 48 h leads to an increase on TMRM fluorescence, possibly indicating an increase on mitochondrial membrane potential. This data seems consistent with the slight increase on TMRM fluorescence also verified for the same time point and concentration on confocal microscopy. A significant increase on TMRM fluorescent signal was also identified on cells treated with 50 μM NEF for 72 h. Despite this data seem to contradict the ones obtained on

confocal microscopy, where the use of 50 µM NEF led to cell depolarization for both time points, this increase on mitochondrial membrane potential may be the result of NEF inhibition on OXPHOS complex V. This hypothesis was already mentioned to explain the small increase on TMRM fluorescence observed onfocal microscopy, after treatment with 20 µM NEF. A temporary blockade of ATP synthase could increase proton accumulation in the intermembrane space, increasing the charge difference between a positively charged intermembrane space and a negatively charged mitochondrial matrix. This hypothesis is supported by published data showing that NEF inhibits complex V (Nadanaciva, Bernal, et al. 2007). However, more experiments are needed to clarify changes on mitochondrial membrane potential after treatment with NEF.

Despite the majority of the data explored until this point suggest that cells treated with NEF undergo cell death, other experiments were performed in order to confirm this. Cells treated with 20 µM and 50 µM for 48 h and 72 h were labelled with CAM and PI and markers fluorescent signal was analysed through flow cytometry (Fig.16 and 17). Results corroborate that NEF induces apoptosis of HepG2 cells. Results revealed a significant increase on permeabilized cells population after treatment with 50 µM NEF for 48 h (Fig.16: A,B) and a significant decrease on live cells. A similar behaviour was observed when the same NEF concentration was used for 72 h (Fig.17-A,B): permeabilized cells increased after NEF treatment while live cells significantly decreased. Cell treatment with NEF at a 20 µM concentration did not change permeabilized or live cells for both time-points tested. This fact can suggest that despite cells treated with 20 µM NEF showed morphological features typical from dead cells, plasmatic membrane still not sufficiently permeabilized to allow PI entrance. However, we also attend that NEF treatment at a 20 µM concentration had a less severe effect on cell mass reduction, cell number, nuclear morphology, ROS generation and alterations on mitochondrial membrane potential. This fact can justify the absence of significant alterations after CAM and PI double-labeling.

The use of CAM and PI provide informations about the effect of NEF in the induction of cell death. However, the assay does not inform about the process involved on cell death triggered by NEF treatment. In order to investigate the activation of apoptosis upon NEF treatment, caspase-3 and 9-like activities were assessed. The assay was performed using the same concentrations tested on previous assays. However, the exposure times tested were

changed for 24 h and 48 h. This change intend to verify if it is possible to find evidence of the occurrence of apoptosis before the 48 h and 72 h treatment times used in previous assays.

After 24h of treatment with NEF (Fig.18), results revealed no changes on caspase 3-like activity in cells treated with 20 µM or 50 µM, comparatively to cells in the control group. On the other hand, differences were found on caspase 9-like activity (Fig. 18) after NEF treatment: cells treated with 20 µM NEF for 24 h showed an increase of caspase 9-like activity, when compared to cells in the control group. This difference confirms the idea that NEF treatment can lead to cell death on a time period lower than 48 h. This data also corroborates the idea that at this time point, NEF triggers the intrinsic apoptotic pathway. As the name suggests, the intrinsic apoptotic pathway is triggered in response to intrinsic signals, such as DNA damage, growth-factor withdrawal and exposure to certain chemotherapeutic agents (Parsons & Green 2010). Once activated, this pathway leads to cell death through outer mitochondrial membrane (OMM) permeabilization, and the release of cyt c to cytoplasm. The association between cyt c, protease-activating factor 1 (APAF-1) and procaspase-9 generates a complex known as "apoptosome", responsible for caspase-9 activation (Zou et al. 1999; Acehan et al. 2002). Taking this information into consideration, the increase on caspase-9-like activity identified in our data is consistent with the hypothesis that the intrinsic apoptotic pathway is activated in response to NEF administration at a concentration of 20 µM, on 24 h of exposure.

When caspase activity was assessed after a period of 48 h of NEF incubation (Fig.19), data showed an increase on caspase 3-like activity on cells treated with both concentrations (20 µM and 50 µM), when compared to cells in the control group. Yet, the comparison of caspase-3-like activity between treated cells and control cells, showed that the most significant increase was verified in cells treated with 20 µM NEF, when both concentrations were compared to the control group. Caspase-9-like activity was also evaluated for this time-point, with results showing a significant increase in cells treated with 20 µM NEF (Fig.19). These data suggest that NEF treatment at this concentration and time-point induces the activation from both extrinsic and intrinsic apoptotic pathways. As explained before, caspase-9 takes part on intrinsic apoptotic pathway. Upon its own activation, the initiator caspase-9 is involved on executor caspase-3 activation, triggering the caspase cascade and subsequent steps of cell death. However, caspase-3 is not only involved on intrinsic apoptotic pathway but also in the extrinsic apoptotic pathway. When cell death is induced through the extrinsic

pathway, the connection between ligands and death receptors leads to receptors oligomerization. This step is followed by the recruitment of adaptor proteins, and caspase activation. One of the caspases activated on this pathway is caspase-8 that can directly activate caspase-3, leading to the following steps of the apoptotic process (Nagata & Golstein 1995; Lee et al. 1997). Caspase-8 can also cleave Bid, producing a truncated form called t-Bid, that is translocated to mitochondria where it promotes cyt c release (Lindsten et al. 2011). Thus, the increase on caspase-3-like activity verified after treatment with 20 µM NEF for 48 h is consistent with extrinsic apoptotic triggering and also reinforces the idea that intrinsic apoptotic pathway is also activated upon NEF treatment, a possibility previously confirmed by the increase in caspase-9-like activity. In order to confirm the activation of the extrinsic pathway of apoptosis, caspase-8-like activity should also be assessed in the future.

As stated above, treatment with 50 µM NEF only significantly increased caspase-3-like activity at a 48 h time-point, while no alterations on caspase-9-like activity were verified. This data support the triggering of intrinsic apoptotic pathway at this concentration and time-point. However, attending that both apoptotic pathways converge on caspase-3, the absence of caspase-9-like activity does not exclude that the extrinsic apoptotic pathway is not triggered on cells treated with 50 µM NEF. This data reinforce the idea that NEF treatment induces cell death and is also consistent with data from previous assays.

A general evaluation about concentrations and time-points tested revealed that the administration of NEF, at 50 µM, had the most severe effects over cell survival and normal cell function, a fact verified over both time-points. The application of this NEF concentration led to a significant decrease in cell mass, compared to the decrease caused by NEF treatment at 20 µM concentration, for each exposure time. Cells treated with 50 µM NEF also exhibited the most deep alterations on nuclear morphology as the higher increase on mitochondrial superoxide anion levels, visible through MitoSOX labeling. In addition, differences permeabilized cells population and live cells population prevalences were only verified on NEF treatment at 50 µM concentration. Analysing this facts,we consider that NEF should not be tested at higher concentrations than 50 µM, avoiding the risk of total cell death. Although NEF treatment at a 50 µM concentration provided interesting results, this treatment showed small effects on caspases activity. However, this fact can be related to a severe toxic effect of NEF on HepG2 cells, that can interfere with caspases activity or even lead to a cell death through a mechanism alternative to apoptosis.

The use of NEF at 20 µM concentration, despite had less severe effects comparatively to 50 µM concentration, discards the risk of higher cell death. The use of this concentration caused a reduction in cell number, ROS increase, changes on mitochondrial membrane potential and apoptosis induction.

Regarding to time points tested in our work, the increase on caspase-9-like activity at the 24h time-point can mean that the apoptotic process starts before the 48h exposure to NEF. Attending to this data, we must perform additional assays, in order to investigate NEF effect on HepG2 cells after 24 h of exposition. Results provided by NEF treatment with both concentrations on 72 h time-point confirmed the majority of the data obtained on 48h and no significant differences resulted from this increase on treatment period to NEF. However, caspases activity should be also evaluated on 72 h of exposure in order to verify if the increase on caspases activity still occurs on a longer exposition period to NEF.

Although we have not confirmed the connection between NEF treatment and p66Shc activation and translocation to mitochondria, we found evidences supporting that NEF treatment increases superoxide anion in mitochondria. Taking this information into consideration, it is possible that NEF trigger apoptosis by p66Shc independent mechanisms. For example, c-Jun N-terminal kinases (JNKs) can be activated upon a stressful stimulus, such as oxidative stress (Wang et al. 2007). Despite the role of JNKs on cyt c release stills unclear, some evidences suggest that this protein takes part on cyt c release, through a pathway involving Bid cleavage (Madesh et al. 2002). The ability of JNK to promote apoptosis can be also related with inhibitory phosphorylation of anti-apoptotic Bcl-2 protein (Yamamoto et al. 1999).

Attending to this hypothesis we cannot exclude the possibility that other mechanisms are involved on apoptotic induction upon NEF treatment. Thus despite the important role of p66Shc on mitochondria function and regulation of biological processes, further experiments are needed to clarify this point.

5. Final conclusion

The hepatotoxic effects of the antidepressant NEF led to the withdrawal of this drug from the pharmaceutical market. Our work confirmed the toxicity of NEF on a hepatocyte model and also proved the ability of NEF to trigger apoptosis.

Upon NEF treatment HepG2 cells suffer mitochondrial depolarization, increase on ROS generation and increase on caspase activity, leading to loss of cells. Treated cells also exhibited morphological features typical from apoptotic cells. All of this information supports the idea that NEF treatment triggers programmed cell death on HepG2 cells.

The main objective of the present work was to investigate the activation of p66Shc signaling pathway upon NEF treatment. The increase on p66Shc total content was consistent with this hypothesis. However, the analysis of total phosphorylated p66Shc revealed a decrease of this form when NEF treatment was applied. Despite we verified that NEF treatment triggers apoptosis on HepG2 cells, the connection between apoptosis and p66Shc ativation and translocation to mitochondrial remains unclear, although we cannot exclude at this point that a fast turn-over rate of the phosphorylated form exists.

6. Future Perspectives

This work investigated a possible link between NEF toxicity and the activation of p66Shc signalling pathway. Despite our results confirmed apoptosis triggering upon NEF treatment, and increased total p66Shc, further experiments are needed.

The use of a cell line to validate this model exhibits several limitations, so the results should be confirmed by performing *in vivo* studies. HepG2 cells have a little or no CYP34A activity (Wilkening et al. 2003), a cellular structure involved on the hepatotoxicity induced by NEF administration. This fact enhances the importance of *in vivo* studies execution.

Another interesting task to complete this work, would be the study of cellular antioxidant defenses after cells exposure to NEF. Therefore, the determination of reduced glutathione/oxidized glutathione (GSH/GSSG) ratio and superoxide dismutase (SOD) levels should be performed.

Total and phosphorylated p66Shc content should be also evaluated on mitochondrial fractions. This analysis would provide more informations about the role of p66Shc on electron transfer, attending that p66Shc acts on mitochondria electron carrier chain.

To clarify the role of p66Shc on NEF hepatotoxicity and cell death, the use of an HepG2 cell line with SHC1 silenced should be also considered. This modified cell line would allow us to verify if the apoptotic process still occurs, in the absence of a p66Shc activated form. All of this tasks would increase the validity of our results.

7. References

Abramov, A.Y., Scorziello, A. & Duchen, M.R., 2007. Three distinct mechanisms generate oxygen free radicals in neurons and contribute to cell death during anoxia and reoxygenation. *The Journal of Neuroscience.*, 27 (5), pp.1129–1138.

Acehan, D., Jiang, X., Morgan, D. G., Heuser, J. E., Wang, X. & Akey, C.W., 2002. Three-dimensional structure of the apoptosome: implications for assembly, procaspase-9 binding, and activation. *Molecular Cell*, 9 (2), pp.423–432.

Alderman, C.P., 1999. Comment: possible interaction between nefazodone and pravastatin. *The Annals of Pharmacotherapy*, 33 (7-8), p.871.

Aranda-Michel, J., Koehler, A., Bejarano, P.A., Poulos, J. E., Luxon, B. A., Khan, C. M., Ee, L. C., Balistreri, W. F. & Weber, F. L., 1999. Nefazodone-induced liver failure: report of three cases. *Annals of Internal Medicine*, 130 (4 Pt 1), pp.285–288.

Arndt-Jovin, D.J. & Jovin, T.M., 1977. Analysis and sorting of living cells according to deoxyribonucleic acid content. *Journal of Histochemistry & Cytochemistry*, 25(7), pp.585-589.

Ashkenazi, A. & Dixit, V.M., 1998. Death receptors: signaling and modulation. *Science*, 281(5381), pp. 1305-1308.

Banki, K., Hutter, E.,Gonchoroff, N.J. & Perl, A., 1999. Elevation of mitochondrial transmembrane potential and reactive oxygen intermediate levels are early events and occur independently from activation of caspases in fas signaling. *Journal of Immunology*, 162(3), pp. 1466–1479.

Benazzi, F., 1997. Dangerous interaction with nefazodone added to fluoxetine, desipramine, venlafaxine, valproate and clonazepam combination therapy. *Journal of Psychopharmacology*, 11 (2), pp.190–191.

Bonfini, L., Migliaccio, E., Pelicci, G., Lanfrancone, L. & Pelicci, PG., 1996. Not all Shc's roads lead to Ras. *Trends in Biochemical Sciences*, 21 (7), pp.257–261.

Bradford, M.M., 1976. A rapid and sensitive method for the quantitation of microgram quantities of protein utilizing the principle of protein-dye binding. *Analytical Biochemistry*, 72, (1), pp. 248-254.

Brenner, D. & Mak, T.W., 2009. Mitochondrial cell death effectors. *Current Opinion in Cell Biology*, 21 (6), pp.871–877.

Bystritsky, A., Rosen, R., Suri, R. & Vapnik, T., 1999. Pilot open-label study of nefazodone in panic disorder. *Depression and Anxiety*, 10 (3), pp.137–139.

Casciola-Rosen, B.L., Nicholson, D. W., Chong, T., Rowan, K. R., Thornberry, N. A., Miller, D. K. & Rosen, A., 1996. Apopain/CPP32 cleaves proteins that are essential for cellular repair: a fundamental principle of apoptotic death. *The Journal of Experimental Medicine*, 183 (5), pp.1957–1964.

Chial, H.J & Splittgerber, A. G, 1993. A comparison of the binding of Coomassie brilliant blue to proteins at low and neutral pH. *Analytical Biochemistry*, 213 (2), pp.362-369.

Choi, S., 2003. Nefazodone (serzone) withdrawn because of hepatotoxicity. *Canadian Medical Association Journal*, 169 (11), p.1187.

Ciraulo, D.A., Shader, R.I. & Greenblatt, D.J., 2010. Clinical pharmacology and therapeutics of antidepressants. In D. A. Ciraulo & R. I. Shader, eds. *Pharmacotherapy of Depression*. Humana Press, pp. 33–124.

CNS forum. The Lundbeck Institute. The mechanism of action of nefazodone (efficacy). Available at: http://www.cnsforum.com/educationalresources/imagebank/antidepressants/drug_nefaz_efficacy. Acessed April 18, 2014.

Cooper, D.M., 2012. The balance between life and death : defining a role for apoptosis in aging. *Journal of Clinical & Experimental Pathology*, S4:001, pp.1–10.

Cory, A. & Adams, J.M., 2002. The BCL2 family: regulators of the cellular life-or-death switch. *Nature Reviews Cancer*, 2 (9), pp.647–656.

Cosentino, F., Francia, P., Camici, G.G., Pelicci, P. Gi., Volpe, M. & Lüscher, T. F., 2008. Final common molecular pathways of aging and cardiovascular disease: role of the p66Shc protein. *Arteriosclerosis, Thrombosis, and Vascular Biology*, 28 (4), pp.622–628.

Cosgrove, B.D., King, B. M., Hasan, M. A., Alexopoulos, L. G., Farazi, P. A., Hendriks, B. S,Griffith, L. G., Sorger, P. K., Tidor, B., Xu, J. J. & Lauffenburger, D.A., 2009. Synergistic drug-cytokine induction of hepatocellular death as an *in vitro* approach for the study of inflammation-associated idiosyncratic drug hepatotoxicity. *Toxicology and Applied Pharmacology*, 237 (3), pp.317–330.

Danial, N.N. & Korsmeyer, S.J., 2004. Cell death : critical control points review. *Cell*, 116 (2), pp.205–219.

Dehn, P.F., White, C. M., Conners, D. E., Shipkey, G. & Cumbo, T. A., 2004. Characterization of the human hepatocellular carcinoma (HepG2) cell line as an *in vitro* model for cadmium toxicity studies. *In Vitro Cellular & Developmental Biology-Animal*, 40 (5-6), pp.172–182.

Dykens, J.A., Jamieson, J. D., Marroquin, L. D., Nadanaciva, S., Xu, J. J. , Dunn, M. C., Smith,A. R., Will, Y., 2008. *In vitro* assessment of mitochondrial dysfunction and cytotoxicity of nefazodone, trazodone, and buspirone. *Toxicological Sciences.*, 103 (2), pp.335–345.

Elmore, S., 2007. Apoptosis: a review of programmed cell death. *Toxicologic Pathology*, 35(4), pp.495–516.

Eloubeidi, M.A., Gaede, J.T. & Swaim, M.W., 2000. Reversible nefazodone-induced liver failure. *Digestive Diseases and Sciences*, 45 (5), pp.1036–1038.

Feighner, J.P., 1999. Mechanism of action of antidepressant medications. *Journal of Clinical Psychiatry*, 60 (suppl 4), pp.4–11.

Giorgio, M., Migliaccio, E., Orsini, F., Paolucci, D., Moroni, M., Contursi, C., Pelliccia, G., Luzi, L., Minucci, S., Marcaccio, M., Pinton, P., Rizzuto, R., Bernardi, P., Paolucci, F. & Pelicci, P.G., 2005. Electron transfer between cytochrome c and p66Shc generates reactive oxygen species that trigger mitochondrial apoptosis. *Cell*, 122 (2), pp.221–233.

Hanahan, D. & Weinberg, R.A., 2000. The hallmarks of cancer. *Cell*, 100 (1), pp.57–70.

Harman, D., 1956. Aging: a theory based on free radical and radiation chemistry. *Journal of Gerontology*, 11 (3), pp.298–300.

He, H. & Richardson, J.S., 1997. Nefazodone: a review of its neurochemical mechanisms, pharmacokinetics, and therapeutic use in major depressive disorder. *CNS Drug Reviews*, 3 (1), pp.34–48.

Hengartner, M.O., 2000. The biochemistry of apoptosis. *Nature*, 407 (6805), pp.770–776.

Hirschfeld, R.M.A., 2000. History and evolution of the monoamine hypothesis of depression. *Journal of Clinical Psychiatry*, 61 (suppl 6), pp.4–6.

Horst, W.D. & Preskorn, S.H., 1998. Mechanisms of action and clinical characteristics of three atypical antidepressants: venlafaxine, nefazodone, bupropion. *Journal of Affective Disorders*, 51 (3), pp.237–254.

Horvitz, H.R., 1999. Genetic control of programmed cell death in the nematode *Caenorhabditis elegans*. *Cancer Research*, 59 (Suppl 7), p.1701s–1706s.

Igney, F.H. & Krammer, P.H., 2002. Death and anti-death: tumour resistance to apoptosis. *Nature Reviews Cancer*, 2 (4), pp.277–288.

Jacobson, M.D., Weil, M. & Raff, M.C., 1997. Programmed cell death in animal development. *Cell*, 88 (3), pp.347–354.

Janicke, R.U., Walker, P. A., Lin, X.Y. & Porter, A. G., 1996. Specific cleavage of the retinoblastoma protein by an ICE-like protease in apoptosis. *The European Molecular Biology Organization Journal*, 15 (24), pp.6969–6978.

Jin, Z. & El-Deiry, W.S., 2005. Overview of cell death signaling pathways. *Cancer Biology & Therapy*, 4 (2), pp.139–163.

Kent, J.M., 2000. SNaRIs , NaSSAs , and NaRIs : new agents for the treatment of depression. *Lancet*, 355 (9207), pp.911–918.

Kerr, J.F.R., Wyllie, A.H. & Currie, A.R., 1972. Apoptosis : a basic biological phenomenon withwide-ranging implications in tissue kinetics. *British Journal of Cancer*, 26 (4), pp.239–257.

Kroemer, G., Dallaporta, B. & Resche-Rigon, M., 1998. The mitochondrial death/life regulator in apoptosis and necrosis. *Annual Review of Physiology*, 60, pp.619–642.

Kurosaka, K., Takahashi, M., Watanabe, N. & Kobayashi, Y.2003. Silent cleanup of very early apoptotic cells by macrophages. *The Journal of Immunology*, 171 (9), pp.4672–4679.

Lazebnik, Y.A., Takahashi, A., Moir, R. D., Goldman, R. D., Poirier, G. G., Kaufmann, S. H. & Earnshaw, W. C., 1995. Studies of the lamin proteinase reveal multiple parallel biochemical pathways during apoptotic execution. *Proceedings of the National Academy of Sciences of the United States of America*, 92 (20), pp.9042–9046.

Lee, J., Richburg, J. H., Younkin, S. C. & Boekelheide, K., 1997. The Fas system is a key regulator of germ cell apoptosis in the testis. *Endocrinology*, 138 (5), pp.2081–2088.

Li, H., Zhu, H., Xu, C.-J. & Yuan, J., 1998. Cleavage of BID by Caspase 8 Mediates the Mitochondrial Damage in the Fas Pathway of Apoptosis. *Cell*, 94 (4), pp.491-501.

Li, P., Nijhawan, D., Budihardjo, I., Srinivasula, S. M., Ahmad, M., Alnemri, E. S. & Wang, X., 1997. Cytochrome c and dATP-dependent formation of Apaf-1/caspase-9 complex initiates an apoptotic protease cascade. *Cell*, 91 (4), pp.479–489.

Lin, Z. & Will, Y., 2012. Evaluation of drugs with specific organ toxicities in organ-specific cell lines. *Toxicological sciences.*, 126 (1), pp.114–127.

Lindsten, T., Ross, A.J. & King, A., 2011. The combined functions of proapoptotic Bcl-2 family members Bak and Bax are essential for normal development of multiple tissues. *Molecular Cell*, 6 (6), pp.1389–1399.

Liu, L.X. & Rustgi, A.K., 1987. Cardiac myonecrosis in hypertensive crisis associated with monoamine oxidase inhibitor therapy. *The American Journal of Medicine*, 82 (5), pp.1060–1064.

Longo-Sorbello, G.S.A., Saydam, G., Banerjee, D. & Bertino, J.R., 2006. Cytotoxicity and cell growth assays. In J. E. Celis, ed. *Cell biology: a laboratory handbook*. Elsevier Academic Press, pp. 315–324.

Lucena, M.I., Andrade, R. J., Gomez-Outes, A., Rubio, M. & Cabello, M. R., 1999. Acute liver failure after treatment with nefazodone. *Digestive Diseases and Sciences*, 44 (12), pp.2577–2579.

Lucena, M.I.,Carvajal, A., Andrade, R.J. & Velasco, A., 2003. Antidepressant-induced hepatotoxicity. *Expert Opinion on Drug safety.*, 2 (3), pp.249–262.

Luzi, L., Carvajal, A., Andrade, R. J. & Velasco, A., 2000. Evolution of Shc functions from nematode to human. *Current Opinion in Genetics & Development*, 10 (6), pp.668–674.

Madesh, M., Antonsson, B., Srinivasula, S. M., Alnemri, E. S. & Hajnóczky, G., 2002. Rapid kinetics of tBid-induced cytochrome c and Smac/DIABLO release and mitochondrial depolarization. *The Journal of Biological Chemistry*, 277 (7), pp.5651–5659.

Mahar, I., Bambico, F. R., Mechawar, N. & Nobrega, J. N. 2014. Stress, serotonin, and hippocampal neurogenesis in relation to depression and antidepressant effects. *Neuroscience and Biobehavioral Reviews*, 38, pp.173–192.

Mennella, M.R., 2011. Mammalian spermatogenesis, DNA repair, Poly (ADO-ribose) turnover: the state of the art. In F. Storici, ed. *DNA Repair- On the Pathways to Fixing DNA Damage and Errors*. INTECH open access publisher.

Migliaccio, E., Giorgio, M., Mele, S., Pelicci, G., Reboldi, P., Pandolfi, P. P., Lanfrancone, L. & Pelicci, P. G.,1999. The p66shc adaptor protein controls oxidative stress response and life span in mammals. *Nature*, 402 (6759), pp. 309-313.

Mikhailov, V., Mikhailova, M., Degenhardt, K., Venkatachalam, M. A., White, E. & Saikumar, P., 2003. Association of Bax and Bak homo-oligomers in mitochondria. Bax requirement for Bak reorganization and cytochrome c release. *The journal of Biological Chemistry*, 278 (7), pp.5367–5376.

Mulinari, S., 2012. Monoamine theories of depression: historical impact on biomedical research. *Journal of the History of the Neurosciences*, 21 (4), pp.366–392.

Nadanaciva, S., Bernal, A., Aggeler, R., Capaldi, R. & Will, Y., 2007. Target identification of drug induced mitochondrial toxicity using immunocapture based OXPHOS activity assays. *Toxicology in Vitro*, 21 (5), pp.902–911.

Nagata, S. & Golstein, P., 1995. The Fas death factor. *Science*, 267 (5203), pp.1449–1456.

Neri, S., Mariani, E., Meneghetti, A., Cattini, L., Facchini, A., 2001. Calcein-Acetyoxymethyl Cytotoxicity assay: standardization of a method allowing additional analyses on recovered effector cells and supernatants. *Clinical and Diagnostic Laboratory Immunology*, 8 (6), pp.1131–1135.

Orsini, F., Migliaccio, E., Moroni, M., Contursi, C., Raker, V. A., Piccini, D., Martin-Padura, I., Pelliccia, G., Trinei, M., Bono, M., Puri, C., Tacchetti, C., Ferrini, M., Mannucci, R., Nicoletti, I., Lanfrancone, L., Giorgio, M. & Pelicci, P. G., 2004. The life span determinant p66Shc localizes to mitochondria where it associates with mitochondrial heat shock protein 70 and regulates trans-membrane potential. *The Journal of Biological Chemistry*, 279 (24), pp.25689–25695.

Pacini, S., Pellegrini, M., Migliaccio, E., Patrussi, L., Ulivieri, C., Ventura, A., Carraro, F. Naldini, A., Lanfrancone, L., Pelicci, P. & Baldari, C. T., 2004. p66SHC promotes apoptosis and antagonizes mitogenic signaling in T cells. *Molecular and Cellular Biology*, 24 (4), pp.1747–1757.

Papazisis, K.T., Geromichalos, G. D., Dimitriadis, K. A. & Kortsaris, A. H., 1997. Optimization of the sulforhodamine B colorimetric assay. *Journal of Immunological Methods*, 208 (2), pp.151–158.

Parsons, M.J. & Green, D.R., 2010. Mitochondria in cell death. *Essays in Biochemistry*, 47, pp.99–114.

Pehar, M., Robinson, K. M., Cassina, P., Díaz-Amarilla, P. J., Hagen, T. M., Radi, R., Barbeito, L. & Beckman, J. S., 2007. Mitochondrial superoxide production and nuclear factor erythroid 2-related factor 2 activation in p75 neurotrophin receptor-induced motor neuron apoptosis. *The journal of Neuroscience.*, 27 (29), pp.7777–7785.

Perry, S.W., Norman, J. P., Barbieri, J., Brown, E. B., Gelbard, H.A., 2011. Mitochondrial membrane potential probes and the proton gradient: a practical usage guide. *Biotechniques.*, 50 (2), pp.98–115.

Petronilli, V., Costantini, P., Scorrano, L., Colonna, R., Passamontil, S. & Bernardi, P.,1994. The voltage sensor of the mitochondrial permeability transition pore is tuned by the oxidation-reduction state of vicinal thiols. Increase of the gating potential by oxidants and its reversal by reducing agents. *The jounal of Biological Chemistry*, 269 (24), pp.16638–16642.

Pinton, P., Rimessi, Al. Marchi, S., Orsini, F., Migliaccio, E., Giorgio, M., Contursi, C., Minucci, S., Mantovani, F., Wieckowski, M. R., Del Sal, G., Pelicci, P. G. & Rizzuto, R., 2007. Protein kinase C beta and prolyl isomerase 1 regulate mitochondrial effects of the life-span determinant p66Shc. *Science*, 315 (5812), pp.659–663.

Raffaello, A. & Rizzuto, R., 2011. Mitochondrial longevity pathways. *Biochimica et Biophysica Acta*, 1813 (1), pp.260–268.

Redmile-Gordon, M.A., Armenise, E., White, R.P., Hirsch, P.R. & Goulding, K.W.T., 2013. A comparison of two colorimetric assays, based upon Lowry and Bradford techniques, to estimate total protein in soil extracts. *Soil biology & Biochemistry*, 67(100), pp.166-173.

Richelson, E., 2001. Pharmacology of antidepressants. *Mayo Clinic Proceedings*, 76 (5), pp.511–527.

Robinson, K.M., Janes, M.S., Pehar, M., Monette, J. S., Ross, M. F., Hagen, T. M., Murphy, M.P. & Beckman, J.S., 2006. Selective fluorescent imaging of superoxide in vivo using ethidium-based probes. *Proceedings of the National Academy of Sciences of the United States of America*, 103 (41), pp.15038–15043.

Roe, A.L., Snawder, J. E., Benson, R. W., Roberts, D. W. & Casciano, D. A., 1993. HepG2 cells: an *in vitro* model for P450-dependent metabolism of acetaminophen. *Biochemical and Biophysical Research Communications*, 190 (1), pp.15–19.

Sampson, D.L., Chng, Y. L., Upton, Z., Hurst, C. P., Parker, A. W. & Parker, T. J., 2013. The highly abundant urinary metabolite urobilin interferes with the bicinchoninic acid assay. *Analytical Biochemistry*, 442 (1), pp.110–117.

Savill, J. & Fadok, V., 2000. Corpse clearance defines the meaning of cell death. *Nature*, 407 (6805), pp.784–788.

Skehan, P. ,Storeng, R., Scudiero, D., Monks, A., McMahon, J., Vistica, D., Warren, J. T., Bokesch, H., Kenney, S. & Boyd, M. R., 1990. New colorimetric cytotoxicity assay for anticancer-drug screening. *Journal of the National Cancer Institute*, 82 (13), pp.1107–1112.

Smith, P.K., Krohn, R. I., Hermansom, G. T., Mallia, A. K., Gartner, F. H., Provenzano, M. D., Fujimoto, E. K., Goeke, N. M., Olson, B. J. & Klenk, D. C., 1985. Measurement of protein using bicinchonicic acid. *Analytical Biochemistry*, 150 (1), pp.76–85.

Taylor, D.P., Smith, D.W., Hyslop, D.K., Riblet, L.A. & Temple, D.L. Jr, 1986. Receptor binding and atypical antidepressant drug discovery. In R. O'Brien, ed. *Receptor binding and drug research*. Marcel Dekker Inc, pp. 151–165.

Taylor, F.B. & Prather, M.R., 2003. The efficacy of nefazodone augmentation for treatment-resistant depression with anxiety symptoms or anxiety disorder. *Depression and Anxiety*, 18 (2), pp.83–88.

Tebourbi, O., Rhouma, K.B. & Sakly, M., 1998. DDT induces apoptosis in rat thymocytes. *Bulletin of Environmental Contamination and Toxicology*, 61 (2), pp.216–223.

Thabrew, M.I., Mitry, R. R, Morsy, M.A. & Hughes, R. D. 2005. Cytotoxic effects of a decoction of *Nigella sativa, Hemidesmus indicus* and *Smilax glabra* on human hepatoma HepG2 cells. *Life Sciences*, 77 (12), pp.1319–1330.

Thompson, C.B., 1995. Apoptosis in the pathogenesis and treatment of disease. *Science*, 267 (5203), pp.1456–1462.

Trump, B.E., Berezesky, I. K., Chang, S. H. & Phelps, P. C., 1997. The Pathways of Cell Death: Oncosis, Apoptosis, and Necrosis. *Toxicologic Pathology*, 25 (1), pp.82–88.

Van IJzendoorn, S.C.D. & Hoekstra, D., 2000. Polarized sphingolipid transport from the subapical compartment changes during cell polarity development. *Molecular Biology of the Cell*, 11 (3), pp.1093–1101

Veeramani, S., Chou, Y.-W., Lin, F. C., Sakthivel, M., Fen-Fen, L., Satyendra, K., Xie, Y. , Lele, S. M., Tu, Y. & Lin, M.-F. 2012. Reactive oxygen species induced by p66Shc longevity protein mediate nongenomic androgen action via tyrosine phosphorylation signaling to enhance tumorigenicity of prostate cancer cells. *Free Radical Biology & Medicine*, 53 (1), pp.95–108.

Vermes, I., Haanen, C., Steffens-Nakken, H. & Reutelingsperger, C., 1995. A novel assay for apoptosis. Flow cytometric detection of phosphatidylserine expression on early apoptotic cells using fluorescein labelled Annexin V. *Journal of Immunological Methods*, 184 (1), pp.39–51.

Von Moltke, L.L., Greenblatt, D. J., Granda, B. W., Grassi, J. M., Schmider, J., Harmatz, J. S. & Shader, R. I.1999. Nefazodone, meta-chlorophenylpiperazine, and their metabolites *in vitro*: cytochromes mediating transformation, and P450-3A4 inhibitory actions. *Psychopharmacology*, 145 (1), pp.113–122.

Wang, F., Murrell, G.A.C. & Wang, M.-X., 2007. Oxidative stress-induced c-Jun N-terminal kinase (JNK) activation in tendon cells upregulates MMP1 mRNA and protein expression. *Journal of Orthopaedic Research.*, 25 (3), pp.378–389.

Wei, M.C., Zong, W.-X, Cheng, E.H-Y., Lindsten, T., Panoutsakopoulou,V., Ross, A.J., Roth, K.A., MacGregor, G.R., Thompson, C.B. & Korsmeyer, S.J., 2001. Proapoptotic BAX and BAK: a requisite gateway to mitochondrial dysfunction and death. *Science*, 292 (5517), pp. 727-730.

Weisenfeld, R.B., 2007. Mass transport kinetics of the DNA-binding dye Hoechst-33342 into bovine spermatozoa. *Bioorganic & Medicinal Chemistry*, 15(19), pp. 6361–6366.

Weston, S.A. & Parish, C.R., 1992. Calcein: a novel marker for lymphocytes which enter lymph nodes. *Cytometry*, 13 (7), pp.739–749.

Wilkening, S., Stahl, F. & Bader, A., 2003. Comparison of primary human hepatocytes and hepatoma cell line HepG2 with regard to their biotransformation properties. *Drug Metabolism and Disposition*, 31 (8), pp.1035–1042.

Willis, S.N., Fletcher, J. I., Kaufmann, T., van Delft, M. F., Chen, L., Czabotar, P.E., Ierino, H., Lee, E. F., Fairlie, W. D., Bouillet, P., Strasser, A., Kluck, R. M., Adams, J. M. Huang, D. C. 2007. Apoptosis initiated when BH3 ligands engage multiple Bcl-2 homologs, not Bax or Bak. *Science*, 315 (5813), pp.856–859.

World Health Organization, Mental Health. Depression. Available at: http://www.who.int/mental_health/management/depression/en/ Accessed February 5, 2014.

Yamamoto, K., Ichijo, H. & Korsmeyer, S.J., 1999. BCL-2 is phosphorylated and inactivated by an ASK1/Jun N-terminal protein kinase pathway normally activated at G2/M. *Molecular and Cellular Biology*, 19 (12), pp.8469–8478.

Youle, R.J., 2007. Cell Biology. Cellular demolition and the rules of engagement. *Science*, 315 (5813), pp.776–777.

Youle, R.J. & Strasser, A., 2008. The BCL-2 protein family: opposing activities that mediate cell death. *Nature Reviews Molecular Cell Biology*, 9 (1), pp.47–59.

Zou, H., Li, Y., Liu, X. & Wang, X., 1999. An APAF-1·cytochrome c multimeric complex is a functional apoptosome that activates procaspase-9. *The Journal of Biological Chemistry*, 274 (17), pp. 11549-11556.